

ALMA MATER STUDIORUM · UNIVERSITY OF BOLOGNA

---

School of Science  
Department of Physics and Astronomy  
Master Degree in Physics

# Black Holes with Rotating Quantum Dust Cores

Supervisor:  
Prof. Roberto Casadio

Submitted by:  
Ediz Yılmaz

Academic Year 2024/2025

## Abstract

Classical gravitational collapse models suggest the existence of spacetime singularities, where one expects Einstein’s general relativity to break down. There are several approaches in the literature to avoid such singularities, by either imposing regularity conditions inspired by classical physics or attempting to give quantum mechanical description to the existing collapse models. Here, we review a recent proposal [1, 2] in which the collapse is modelled as a dust ball with a sequence of layers. By quantising the trajectories of dust particles in each layer, one finds a collective ground state for the core which has a radius of  $\frac{3}{2}G_NM$ , thus supporting the idea that black holes can be macroscopic extended objects. We then discuss the effects of rotation on the core by following the analysis in [3], which shows that increasing (classical) angular momentum increases the core radius but corresponds to a smaller outer horizon while removing the inner horizon completely within the perturbative approximation. Finally, we repeat a similar analysis for a more “realistic” case in which we consider the geometry to be described by the Kerr metric and observe that it yields similar results.

# Contents

<b>Introduction</b>	<b>1</b>
<b>1 Classical gravitational collapse and black holes</b>	<b>4</b>
1.1 Stellar evolution in a nutshell . . . . .	4
1.2 Static sphere of fluid . . . . .	6
1.2.1 The interior solution . . . . .	6
1.2.2 The Buchdahl limit . . . . .	10
1.3 Gravitational collapse of a ball of dust . . . . .	13
1.3.1 Lemaître-Tolman-Bondi model . . . . .	13
1.3.2 Oppenheimer-Snyder model . . . . .	15
1.4 Black holes . . . . .	17
1.4.1 Contracting beyond $r = 2G_N M$ . . . . .	17
1.4.2 The singularity . . . . .	19
1.5 Rotating black holes . . . . .	22
1.5.1 The Kerr solution . . . . .	22
1.5.2 Horizons . . . . .	22
1.5.3 Frame dragging and the ergosphere . . . . .	23
1.5.4 The singularity of Kerr spacetime . . . . .	24
<b>2 Quantum ball of dust</b>	<b>26</b>
2.1 Collapse of a quantum ball of dust . . . . .	27
2.1.1 Quantisation . . . . .	29
2.1.2 A lower bound . . . . .	30
2.2 Ground state layers . . . . .	31
2.2.1 Effective energy density and pressures . . . . .	33
<b>3 Quantum dust layers of rotating black holes</b>	<b>35</b>
3.1 Rigidly rotating ball with classical angular momentum . . . . .	35
3.1.1 Outer geometry . . . . .	37
3.1.2 Angular momentum quantisation . . . . .	38
3.2 General relativistic treatment . . . . .	39

3.2.1	Rotating geodesics . . . . .	39
3.2.2	Ground state and perturbative spectrum . . . . .	41
3.2.3	Slow-rotation . . . . .	42
3.2.4	Quantised specific angular momentum . . . . .	44
<b>Conclusions</b>		<b>45</b>
<b>A Curvature quantities</b>		<b>47</b>
A.1	Spherically symmetric spacetime . . . . .	47
A.1.1	Comoving coordinates . . . . .	48
<b>B Geodesics</b>		<b>49</b>
B.1	Radial geodesics in Schwarzschild spacetime . . . . .	49
B.2	Geodesics of Kerr spacetime . . . . .	52
<b>Bibliography</b>		<b>55</b>

# Introduction

Between the 1930s and 1940s Robert Oppenheimer, Richard C. Tolman, and their collaborators showed that at the end of their lives, sufficiently massive stars will collapse indefinitely into a singular configuration [4, 5, 6, 7]. Einstein’s general theory of relativity predicts that such processes produce a black hole geometry characterised by the existence of an event horizon. Once the horizon forms, the interior becomes geodesically incomplete and contains a spacetime singularity, whose existence was proved by Stephen W. Hawking and Roger Penrose in the late 1960s [8, 9].

The singularity is a “region” that contains a finite amount of mass within zero proper volume, where the tidal forces diverge. The prediction of such singularities clearly suggests a breakdown of general relativity in its original formulation since the classical description of matter cannot be expected to remain valid at such extreme conditions. The singularity theorems of Hawking and Penrose do not prove that the singularities in classical general relativity have infinite spacetime curvature, however, they strongly suggest that at these extreme conditions, as in gravitational collapse, the quantum mechanical effects cannot be ignored.

Although these quantum effects are usually associated with processes that occur at the Planck mass  $m_p$  and length  $\ell_p$ , processes that involve bound states occur at significantly larger length scales. We recall that, the way quantum mechanics explains the stability of atoms and resolves the ultraviolet catastrophe, is by not admitting quantum states corresponding to classical trajectories of the electron around the nucleus. In a similar way, it is expected [10] that quantum mechanics will fix the inconsistencies of the semiclassical approach at the singularity, where the uncertainty principle is clearly violated, and it is conjectured that the singularity will be replaced by a matter core with finite size. Since the quantum description of bound states is not compatible with the background field approach, as in the case of the hydrogen atom, it is suspected that a proper quantum theory of black holes might require a new perspective in which the classical geometry might emerge as an effective field description.

Since objects of compactness  $X = G_N M / R_S \sim 1$ , where the quantum effects are expected to become relevant, occur in nature only at processes with matter sources of several solar masses and thus  $\sim 10^{57}$  neutrons, it is practically impossible to model their gravitational collapse in detail. Therefore, the usual approach is to consider simplified

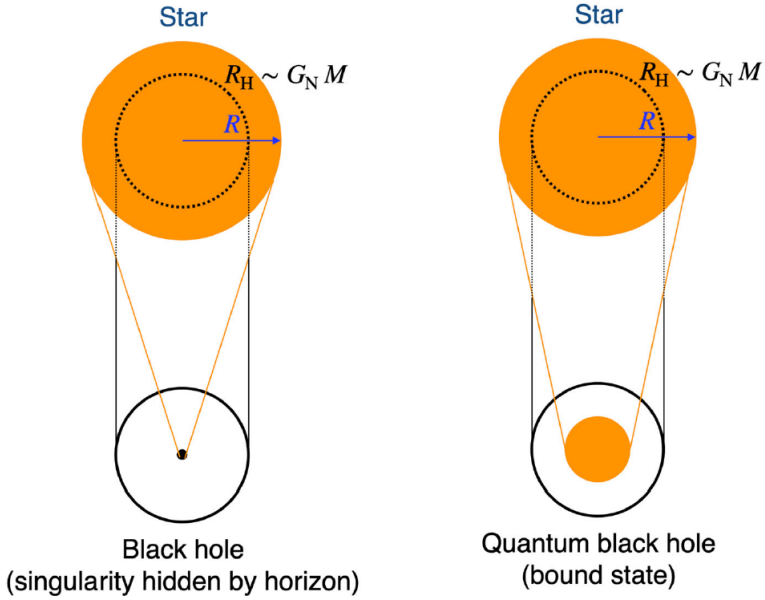


Figure 1: Black hole formation in classical general relativity versus quantum gravity (from [10]).

toy models that allow for analytical treatment, like the Lemaître-Tolman-Bondi and the Oppenheimer-Snyder models, and attempt to give a quantum mechanical description.

Many of these attempts in the literature start from a reduction of degrees of freedom using the spherical symmetry and continuity of the fluid that describes the dust configuration. This uniquely determines the solutions both inside (LTB) and outside (Schwarzschild). From the Einstein-Hilbert action, one can identify a few collective degrees of freedom, particularly the radius  $R_S = R_S(\tau)$ , the Schwarzschild coordinate time  $T_S = T_S(\tau)$  of the dust ball, and the ADM mass  $M$  [11]. Then these collective degrees of freedom can be analysed in the Hamiltonian formalism and canonically quantised [12, 13, 14].

The problem with the approach mentioned above becomes clear when the following is realised: The thermodynamics of perfect fluids, i.e. properties like pressure, temperature, and volume, are derived *a posteriori* from the statistical mechanics of classical particles in a canonical ensemble. This is also true for fermions and bosons which are quantum particles themselves. However, the quantum equation of state of a gas is obviously not obtained by quantising the collective pressure, density, and volume of the gas. With this in mind, and considering the system to which we are trying to provide a quantum description consists of many particles, it seems logical to conclude that it is those particles that require a proper quantum description to begin with and not the ball as a whole.

An alternative approach [1, 2], which is the main guideline of this dissertation and

is reviewed in chapter 2, is to describe the ball of dust as the quantum state of a very large number of particles of mass  $\mu \ll M$  and eventually derive a collective, fluid-like description a posteriori.

The outline of this thesis is as follows:

## Chapter 1

We first discuss the equilibrium conditions of stars, as modelled by a spherically symmetric perfect fluid, mainly from a general relativistic point of view. Then we introduce the standard classical gravitational collapse models, namely, the Lemaître-Tolman-Bondi and the Oppenheimer-Snyder models. We end the chapter with a brief summary of space-time singularities, mentioning the famous singularity theorems of Hawking and Penrose, and the Kerr solution for rotating black holes.

## Chapter 2

We review the alternative quantisation procedure for the gravitational collapse of a ball of dust analysed in [1, 2]. The key idea is to divide the dust ball into  $N$  concentric layers, and quantise the geodesic equation for the areal radius for each layer as an effective quantum mechanical description of the ball as in the case of the usual quantum mechanical description of the hydrogen atom. This approach leads to the existence of a discrete spectrum of bound states, and one finds that the dust ball in its ground state has a quantised and macroscopically large surface area, hence no singularity ever forms.

## Chapter 3

Here we investigate the effects of rotation on the dust core of the black hole as modelled in the previous chapter. First, we treat the core as a slowly rotating rigid ball with classical angular momentum and use perturbation theory to calculate the energy eigenvalues and the core radius as corrections to the static case, as analysed in [3]. Then, we attempt to extend this approach to a more realistic case by considering a full general relativistic treatment in which the spacetime geometry is described by the Kerr solution.

# Chapter 1

## Classical gravitational collapse and black holes

The purpose of this first chapter is to introduce classical general relativistic models of gravitational collapse in the way it was first established by the pioneers R. Oppenheimer, H. Snyder, R. Tolman, G. Lemaître, and H. Bondi. We also review the evolutionary phases and equilibria of spherically symmetric fluids to see under what conditions collapse occurs. We conclude the chapter by briefly discussing the consequences of a complete gravitational collapse and some properties of rotating black holes.

### 1.1 Stellar evolution in a nutshell

Stars are born when fragments of primordial hydrogen clouds with enough mass contract under their own gravity and start fusing hydrogen into heavier elements. With mass  $M \gtrsim 0.08M_\odot$ , the core temperature reaches around  $4 \times 10^6 K$ , which is high enough to start the fusion of hydrogen into helium. During this stage of the star's lifetime, which is called the *main-sequence*, it is in a state of equilibrium under the gravitational attraction and the outward thermal pressure by the nuclear reactions. When the star exhausts its hydrogen fuel in its core, it cools down, and its gravity causes it to contract further. Thus, the star exits the main-sequence and its evolution depends on its mass.

One of the possible end stages of stellar evolution is a *white dwarf*. It is a compact remnant of a star that has used all of its fuel and stopped nuclear fusion. They have masses around  $\sim 1 M_\odot$  and radius comparable to that of the Earth, so their average density is of the order of  $\bar{\rho} \sim 10^6 \text{ g/cm}^3$  ( $\bar{\rho}_\odot = 1.4 \text{ g/cm}^3$  for comparison). In the 1930s, it was found by Chandrasekhar [15] that a star cannot form a stable white dwarf if its mass is greater than  $1.44 M_\odot$ , which is famously known as the *Chandrasekhar limit*.

Stars with mass  $M \lesssim 0.5 M_\odot$  form a white dwarf without intermediate stages. More massive stars, with mass between  $0.5 M_\odot$  and  $8 - 10 M_\odot$ , can fuse helium to produce

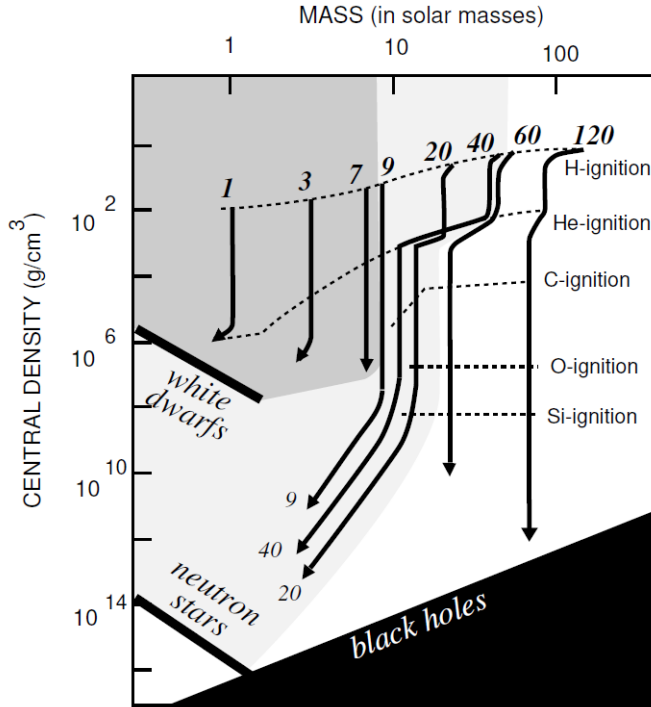


Figure 1.1: Density-mass diagram of astronomical objects (from [16])

carbon and oxygen, contracting even further at each step, raising the temperature and pressure in the core, allowing nuclear processes to produce the next element. However, stars in this mass range cannot produce elements heavier than oxygen. Thus, when they exhaust all their fuel, they contract until they also become a white dwarf.

If the star has a mass between  $8M_{\odot}$  and  $20 - 30M_{\odot}$ , its evolutionary path will be different: The gravitational attraction will become strong enough to overcome the internal pressure, and the core will collapse in a fraction of a second. During this process, electrons are forced to merge with protons to produce neutrons, and the core reaches densities of the order of atomic nuclei, i.e.  $\sim 10^{14}$  g/cm<sup>3</sup>. This core is now so rigid that the infalling matter bounces back to produce a violent shock wave, called a *supernova*, that ejects the external matter into outer space, leaving behind a *neutron star* with a mass around  $M \sim 1 - 3 M_{\odot}$  and a radius of 10 – 15 km, which is kept together by the quantum mechanical pressure of the degenerate Fermi gas of neutrons.

The final possible end stage for a star is reached when the mass of the neutron star exceeds the so called *Tolman-Oppenheimer-Volkoff limit* [5, 7], which is around  $3M_{\odot}$ , above which the star would not be stable and collapse to a point-like singularity to form a *black hole*.

## 1.2 Static sphere of fluid

Before dealing with gravitational collapse, we will briefly discuss the equilibrium conditions of spherically symmetric perfect fluids from a general relativistic perspective to see under what conditions collapse occurs. To do that, we first need to determine the gravitational field inside a static, spherically symmetric fluid.

### 1.2.1 The interior solution

Since we are looking for a static, spherically symmetric solution, we consider the most general metric in the form

$$ds^2 = -e^{\nu(r)}dt^2 + e^{\lambda(r)}dr^2 + r^2(d\theta^2 + \sin^2\theta d\phi^2) \quad (1.1)$$

where functions  $\nu$  and  $\lambda$  are independent of time and will be determined according to the interior structure of the star. A good way to model this internal structure is by assuming that the matter can be described as a perfect fluid with the energy-momentum tensor

$$T^{\mu\nu} = (\rho + p)u^\mu u^\nu + pg^{\mu\nu} \quad (1.2)$$

where  $\rho(r)$  is the proper energy density,  $p(r)$  is the isotropic pressure in the co-moving frame, and  $u^\mu$  is the 4-velocity of the fluid. Since we are dealing with a static configuration, we only have the  $u^0$  component;

$$u^\mu = (e^{-\nu/2}, 0, 0, 0). \quad (1.3)$$

Now, substituting the energy-momentum tensor given above into the Einstein field equations, and using the Ricci scalar and the nonzero components of the Ricci tensor (see Appendix A), we see that the Einstein equations yield 3 equations;

$$G^0_0 = -e^{-\lambda} \left[ \frac{\lambda'}{r} - \frac{1}{r^2} \right] - \frac{1}{r^2} = -8\pi G_N \rho \quad (1.4)$$

$$G^1_1 = e^{-\lambda} \left[ \frac{\nu'}{r} + \frac{1}{r^2} \right] - \frac{1}{r^2} = 8\pi G_N p \quad (1.5)$$

$$G^2_2 = e^{-\lambda} \left[ \frac{\nu''}{2} + \frac{\nu'^2}{4} - \frac{\nu'\lambda'}{4} + \frac{(\nu' - \lambda')}{2r} \right] = 8\pi G_N p \quad (1.6)$$

where  $f' = \partial_r f$  for any function  $f$ . We can write Eq. (1.4) as

$$8\pi G_N \rho r^2 = 1 - (e^{-\lambda} r)', \quad (1.7)$$

which can be integrated to find one of the metric functions

$$e^{-\lambda} = g^{rr} = 1 - \frac{2G_N m(r)}{r} \quad (1.8)$$

where  $m(r)$  is the (Misner-Sharp-Hernandez) *mass function* [17, 18], defined as

$$m(r) = 4\pi \int_0^r \rho(x)x^2 dx, \quad (1.9)$$

such that the total mass of a star of radius  $r = R_S$  is given by  $M = m(R_S)$ , which is also the ADM mass of the system which appears in the exterior Schwarzschild solution. The mass function  $m(r)$  can also be interpreted as the total mass contained within a sphere of (coordinate) radius  $r$ .

Now, the conservation equation  $\nabla_\mu G^{\mu\nu} = \nabla_\mu T^{\mu\nu} = 0$  implies

$$\nabla_\mu [(\rho + p)u^\mu u^\nu + pg^{\mu\nu}] = 0. \quad (1.10)$$

Using the fact that we are dealing with a static distribution of matter, this reduces to

$$p_{,\mu} - (\rho + p)\Gamma_{\mu\nu}^\lambda u_\lambda u^\nu = 0 \quad (1.11)$$

$$p_{,r} - (\rho + p)\Gamma_{14}^4 u_4 u^4 = 0 \quad (1.12)$$

which yields

$$p' = -\frac{\nu'}{2}(\rho + p). \quad (1.13)$$

Now using this equation to substitute  $\nu'$  in the field equation (1.5), and using the metric function  $e^{-\lambda}$  we found, we obtain a differential equation for  $p$ ;

$$p'(r) = -[\rho(r) + p(r)]\frac{G_N}{r^2} [m(r) + 4\pi r^3 p] \left[1 - \frac{2G_N m(r)}{r}\right]^{-1} \quad (1.14)$$

or equivalently,

$$p'(r) = -\rho(r)\frac{G_N m(r)}{r^2} \left[1 + \frac{p(r)}{\rho(r)}\right] \left[1 + \frac{4\pi r^3 p(r)}{m(r)}\right] \left[1 - \frac{2G_N m(r)}{r}\right]^{-1} \quad (1.15)$$

This is called the **Tolman-Oppenheimer-Volkoff** (TOV) equation [5]. From the latter equation, it can easily be seen that this is just the Newtonian equation for hydrostatic equilibrium with general-relativistic corrections supplied by the last three factors. Indeed, in the non-relativistic limit  $|\frac{p}{c^2}| \ll \rho$  and the weak field limit  $G_N m(r) \ll r$ , it reduces to

$$p'(r) \simeq -\rho(r)\frac{G_N m(r)}{r^2}. \quad (1.16)$$

Comparing this with the TOV equation, we observe that, due to the general relativistic correction factors, the magnitude of  $p'(r)$  given by the TOV equation, is always greater than the Newtonian counterpart. This implies that, in general relativity, a higher central pressure,  $p_c$ , is needed to maintain equilibrium than in Newtonian theory.

Now to solve the TOV equation, we need we need to specify an equation of state. For now, we consider the simplest case, where the density  $\rho(r)$  is constant,

$$\rho(r) = \rho_0, \quad (1.17)$$

for  $0 \leq r \leq R_S$ , where  $R_S$  is the radius of the star. Then Eq. (1.8) becomes

$$e^{-\lambda} = 1 - \frac{2G_N m(r)}{r} = 1 - \frac{8\pi G_N \rho_0}{3} r^2 \equiv 1 - Ar^2 \quad (1.18)$$

where  $A = \frac{8\pi G_N \rho_0}{3}$ . Since  $\rho$  is constant, we can write equation (1.13) in the form

$$(\rho_0 + p)' = -\frac{\nu'}{2}(\rho_0 + p) \quad (1.19)$$

and integrating it gives

$$(\rho_0 + p) = B e^{-\nu/2} \quad (1.20)$$

where  $B$  is an integration constant, which will be determined by the matching conditions. Now using the field equations (1.4) and (1.5), we get

$$G^1_1 - G^0_0 = e^{-\lambda} \frac{(\lambda' + \nu')}{r} = 8\pi G_N (\rho_0 + p). \quad (1.21)$$

Substituting the expressions we found for  $e^{-\lambda}$  and  $e^{-\nu/2}$  into Eq. (1.21),

$$\begin{aligned} e^{-\lambda} \left( \frac{2A r e^\lambda + \nu'}{r} \right) &= 8\pi G_N B e^{-\nu/2} \\ e^{\nu/2} \left[ 2Ar + (1 - Ar^2)\nu' \right] &= 8\pi G_N B r \end{aligned}$$

and observing that  $[e^{\nu/2}(1 - Ar^2)^{-1/2}]' = \frac{\nu' e^{\nu/2}}{2}(1 - Ar^2)^{-1/2} + \frac{e^{\nu/2}}{2} 2Ar(1 - Ar^2)^{-3/2}$ , the left hand side becomes

$$2(1 - Ar^2)^{3/2} [e^{\nu/2}(1 - Ar^2)^{-1/2}]' = 8\pi G_N B r, \quad (1.22)$$

which can finally be integrated to find

$$e^{\nu/2} = \frac{8\pi G_N B}{2A} - D \sqrt{(1 - Ar^2)}, \quad (1.23)$$

where  $D$  is, again, an integration constant.

To determine the complete solution, we need to connect the interior and exterior Schwarzschild solutions at the surface of the star. Thus, we require that the metric is

continuous at  $r = R_S$ , and impose the condition that  $p(r) = 0$  at the surface. Using Eqs. (1.20), (1.23), and writing  $\rho_0$  in terms of  $A$ , we can write the pressure as

$$\begin{aligned} p(r) &= B e^{-\nu/2} - \rho_0 \\ &= \frac{1}{\kappa} [\kappa B e^{-\nu/2} - 3A] \\ &= \frac{1}{\kappa} \left[ \frac{3AD\sqrt{1-Ar^2} - \frac{\kappa B}{2}}{\frac{\kappa B}{2A} - D\sqrt{1-Ar^2}} \right] \end{aligned} \quad (1.24)$$

where we let  $\kappa \equiv 8\pi G_N$  to avoid clutter. So, matching the metric functions of the interior and the exterior Schwarzschild solution at the surface, we obtain

$$1 - AR_S^2 = 1 - \frac{2G_N M}{R_S}, \quad (1.25)$$

and

$$\left( \frac{8\pi G_N B}{2A} - D\sqrt{1-AR_S^2} \right)^2 = 1 - \frac{2G_N M}{R_S}, \quad (1.26)$$

and the condition that  $p(R_S) = 0$ , using Eq. (1.24), gives

$$3AD\sqrt{1-AR_S^2} = \frac{8\pi G_N B}{2}. \quad (1.27)$$

Eq. (1.25) gives

$$M = \frac{A}{2}R_S^3 = \frac{4}{3}\pi R_S^3 \rho_0, \quad (1.28)$$

and solving Eqs. (1.26) and (1.27), determines the integration constants  $B$  and  $D$ ;

$$B = \frac{3A}{\kappa}\sqrt{1-AR_S^2} = \rho_0\sqrt{1-\frac{8\pi G_N \rho_0}{3}R_S^2} = \rho_0\sqrt{1-\frac{2G_N M}{R_S}} \quad (1.29)$$

$$D = \frac{1}{2}. \quad (1.30)$$

Thus, finally we have constructed the *interior Schwarzschild solution* for a static, spherically symmetric star with constant mass density  $\rho_0$ , which reads

$$ds^2 = - \left[ \frac{3}{2}\sqrt{1-\frac{2G_N M}{R_S}} - \frac{1}{2}\sqrt{1-\frac{2G_N M r^2}{R_S^3}} \right]^2 dt^2 + \frac{dr^2}{\left(1-\frac{2G_N M}{R_S^3}\right)r^2} + r^2 d\Omega^2 \quad (1.31)$$

where  $d\Omega^2 = (d\theta^2 + \sin^2 \theta d\phi^2)$  is the usual 2-sphere line element, and the pressure is given by

$$p(r) = \rho_0 \frac{\sqrt{1-\frac{2G_N M}{R_S^3}r^2} - \sqrt{1-\frac{2G_N M}{R_S}}}{3\sqrt{1-\frac{2G_N M}{R_S}} - \sqrt{1-\frac{2G_N M}{R_S^3}r^2}}. \quad (1.32)$$

An interesting feature of the interior Schwarzschild solution, and one of the important differences between Newtonian and general relativistic equilibrium configurations, is that while in Newtonian theory the central pressure  $p_c$  is finite for all values of  $\rho_0$ , which can be seen by integrating Eq. (1.16),

$$p_0 = p_c = \frac{2\pi}{3} \rho_0 G_N R_S^2 \quad (1.33)$$

this is not the case in general relativity. In that case, at the center of the star where  $p$  reaches its maximum value, it becomes

$$p_c = \rho_0 \frac{1 - \sqrt{1 - \frac{2G_N M}{R_S}}}{3\sqrt{1 - \frac{2G_N M}{R_S}} - 1}. \quad (1.34)$$

From this, we can see that the pressure becomes infinite and the solution does not make sense when

$$R_S = \frac{9}{4} G_N M. \quad (1.35)$$

This means that, a uniform density star of mass  $M$  cannot be in equilibrium and will have no regular interior solution, if  $R_S < \frac{9}{4} G_N M$ .

### 1.2.2 The Buchdahl limit

Having dealt with the simplest case of constant mass density, we now want to see if general relativity imposes an absolute upper limit for the mass of a static, spherically symmetric star with arbitrary rest mass density  $\rho(r)$ , irrespective of the equation of state. To do this, we first make the following assumptions:

- the pressure vanishes at the surface of the star, i.e.,  $p(R_S) = 0$ , and is finite at  $r = 0$ ,
- $\rho(r) = 0$  for  $r > R_S$ ,
- the density  $\rho(r)$  must not increase outwards, i.e.,

$$\rho'(r) \leq 0, \quad (1.36)$$

- the mass  $M$  is fixed, so

$$m(R_S) = \int_0^{R_S} 4\pi x^2 \rho(x) dx = M \quad (1.37)$$

where  $M$  is the ADM mass appearing in the exterior Schwarzschild solution.

Now, we want to derive a condition for the maximum mass that complies with the above requirements. By writing the field equation Eq. (1.5) in the form

$$\frac{\nu'}{r} \left( 1 - \frac{2m}{r} \right) - \frac{2m}{r^3} = 8\pi G_N p, \quad (1.38)$$

and using Eq. (1.13),  $\nu' = -2p'/(p(r) + \rho(r))$ , we can eliminate  $p$  and after rearranging, we obtain

$$\frac{d}{dr} \left[ \frac{1}{r} \sqrt{1 - \frac{2G_N m(r)}{r}} \frac{d\zeta(r)}{dr} \right] = \frac{G_N}{\sqrt{1 - \frac{2G_N m(r)}{r}}} \frac{d}{dr} \left( \frac{m(r)}{r^3} \right) \zeta(r), \quad (1.39)$$

where we defined  $\zeta^2(r) \equiv e^\nu$ . Using the matching condition for the  $e^\nu$  to the exterior solution, we can find the initial conditions at  $r = R_S$ :

$$\zeta(R_S) = \left[ 1 - \frac{2G_N M}{R_S} \right]^{1/2}, \quad (1.40)$$

$$\zeta'(R_S) = \frac{G_N M}{R_S^2} \left[ 1 - \frac{2G_N M}{R_S} \right]^{-1/2}. \quad (1.41)$$

Looking at Eq. (1.39), we can observe the following:  $\frac{m(r)}{r^3}$  is the average mass density within the radius  $r$ , and for condition (1.36) to be satisfied, it cannot increase with  $r$ . Also,  $\zeta(r)$  must be positive, otherwise, the pressure will have a singularity when  $\zeta$  passes through zero. Thus, we can say that the right-hand side of equation (1.39) is negative, giving

$$\frac{d}{dr} \left[ \frac{1}{r} \sqrt{1 - \frac{2G_N m(r)}{r}} \frac{d\zeta(r)}{dr} \right] \leq 0. \quad (1.42)$$

Integrating this from  $r$  to  $R_S$  and using the initial condition (1.41), we get

$$\zeta'(r) \geq \frac{G_N M r}{R_S^3} \left[ 1 - \frac{2G_N m(r)}{r} \right]^{-1/2}. \quad (1.43)$$

Integrating again, from 0 to  $R_S$  and using the initial condition for  $\zeta(R_S)$ ,

$$\zeta(0) \leq \sqrt{1 - \frac{2G_N M}{R_S}} - \frac{G_N M}{R_S^3} \int_0^{R_S} \frac{r dr}{(1 - 2G_N m(r)/r)^{1/2}}. \quad (1.44)$$

Now, since we look for an upper bound for  $\zeta(0)$ , we focus on the second term on the right-hand side. This term is smallest when  $m(r)$  is as small as possible. But, because

of the condition  $\rho'(r) \leq 0$ ,  $m(r)$  cannot be smaller than the value it would have for a uniform density star, which means

$$m(r) \geq M \frac{r^3}{R_S^3}. \quad (1.45)$$

Therefore, the right-hand side of Eq. (1.44) is largest when the equality holds in Eq. (1.45). Using this in the integral gives

$$\begin{aligned} \zeta(0) &\leq \sqrt{1 - \frac{2G_N M}{R_S} - \frac{G_N M}{R_S^3} \int_0^{R_S} \left(1 - \frac{2G_N M r^2}{R_S^3}\right)^{-1/2}} \\ &= \frac{3}{2} \sqrt{1 - \frac{2G_N M}{R_S}} - \frac{1}{2} \end{aligned} \quad (1.46)$$

Thus, the condition that  $\zeta(r)$  must be positive definite implies that

$$\sqrt{1 - \frac{2G_N M}{R_S}} \geq \frac{1}{3}, \quad (1.47)$$

that is,

$$R_S \geq \frac{9}{4} G_N M \equiv R_B \quad (1.48)$$

where  $R_B$  is the *Buchdahl limit* [19]. This limit is what we have already found previously for the constant density case. So what we have found out now is that this holds for any star regardless of its mass distribution, as long as it is isotropic and its mass density does not increase outwards.

## 1.3 Gravitational collapse of a ball of dust

The Buchdahl limit tells us that a star with  $R_S < R_B$  cannot be stable. The moment a star passes this limit, any increase in the pressure adds to the gravitational field more than it counteracts it. Hence, gravitational attraction becomes dominant, and unless it loses enough mass by ejecting matter or radiation, then there is now nothing to stop the star from contracting indefinitely, i.e., beyond the Schwarzschild radius  $r = 2G_N M$  and towards the  $r = 0$  singularity where it suffers a complete gravitational collapse.

In this section, we will review a quantitative description of a simplified collapse model [20], which is the result of works by Lemaître, Tolman, Oppenheimer and their collaborators in the 1930's and 1940's [4, 6, 21, 22]. The required simplification is that we consider a spherically symmetric fluid to consist of pressureless dust particles, i.e., we take  $p = 0$ . This allows the model to be solved exactly, and gives a good description for collapsing stars, even though physically realistic configurations include pressure.

We first consider the general case of inhomogeneous models, giving the Tolman solution. Then we finally present the Oppenheimer-Snyder model which makes a further simplification by assuming a constant mass density.

### 1.3.1 Lemaître-Tolman-Bondi model

The analysis of this collapsing model is done by considering the system in comoving coordinates, hence putting the line element in the form:

$$ds^2 = -d\tau^2 + e^{\lambda(\tau, R)} dR + r^2(\tau, R)(d\theta^2 + \sin^2 \theta d\phi^2) \quad (1.49)$$

where  $\tau$  is the proper time of a particle at rest in this coordinate system,  $r$  is the areal radius and  $R$  is just the comoving coordinate. Since we are dealing with a pressureless fluid configuration (dust), the energy-momentum tensor has the form

$$T^{\mu\nu} = \rho u^\mu u^\nu. \quad (1.50)$$

In the comoving coordinates  $u^\mu = (1, 0, 0, 0)$ , so  $T^{\mu\nu}$  has a single non-vanishing component,

$$T^0_0 = -\rho(\tau, R) \quad (1.51)$$

Using the components of the Ricci tensor (see Appendix A) for the metric Eq.(1.49), we can write the field equations in the form:

$$G^0_0 = \frac{e^{-\lambda}}{r^2} (2rr'' + r'^2 - rr'\lambda') - \frac{1}{r^2} (rr'\dot{\lambda} + \dot{r}^2 + 1) = -8\pi G_N \rho, \quad (1.52)$$

$$G^1_1 = e^{-\lambda} r'^2 - 2r\ddot{r} - \dot{r}^2 - 1 = 0, \quad (1.53)$$

$$G^2_2 = G^3_3 = \frac{e^{-\lambda}}{r} (2r'' - r'\lambda') - \frac{\dot{r}\dot{\lambda}}{r} - \ddot{\lambda} - \frac{\dot{\lambda}^2}{2} - \frac{2\ddot{r}}{r} = 0, \quad (1.54)$$

$$G_{01} = R_{01} = 2\dot{r}' - \dot{\lambda}r' = 0 \quad (1.55)$$

where  $\dot{f} \equiv \frac{\partial f}{\partial \tau}$  and  $f' \equiv \frac{\partial f}{\partial R}$ . Integrating Eq.(1.55) we get

$$e^\lambda = \frac{r'^2}{1 - \varepsilon f^2(R)}, \quad \varepsilon = 0, \pm 1. \quad (1.56)$$

where  $f(R)$  is an arbitrary function. Using this in Eq.(1.53) gives

$$2\ddot{r}r + \dot{r}^2 = -\varepsilon f^2(R). \quad (1.57)$$

If we let  $u = \dot{r}^2$ , this equation can be simplified to  $d(ru)/dr = -\varepsilon f^2(R)$ , which can be solved to obtain

$$\dot{r}^2 = -\varepsilon f^2(R) + \frac{F(R)}{r} \quad (1.58)$$

where  $F(R)$  is another arbitrary function. This can be integrated by introducing a parameter  $\eta$  such that  $d\eta = (f/r)d\tau$ . Then, Eq.(1.60) becomes

$$\left(\frac{\partial r}{\partial \eta}\right)^2 = \frac{F}{f^2}r - \varepsilon r^2, \quad (1.59)$$

whose solutions are

$$r = \frac{F(R)}{2f^2(R)}(1 - \cos \eta), \quad \tau - \tau_0(R) = \frac{F(R)}{2f^3(R)}(\eta - \sin \eta), \quad (\text{for } \varepsilon = +1) \quad (1.60)$$

and

$$r = \frac{F(R)}{2f^2(R)}(\cosh \eta - 1), \quad \tau - \tau_0(R) = \frac{F(R)}{2f^3(R)}(\sinh \eta - \eta), \quad (\text{for } \varepsilon = -1) \quad (1.61)$$

while the solution for  $\varepsilon = 0$  can be obtained by solving Eq.(1.58) directly, which gives

$$r = \left(\frac{9F(R)}{4}\right)^{1/3} [\tau - \tau_0(R)]^{2/3} \quad (\text{for } \varepsilon = 0) \quad (1.62)$$

where  $\tau_0(R)$  is again an arbitrary function. Additionally, using Eq. (1.58) in Eq. (1.56) we can eliminate  $f^2$  and obtain an expression for the energy density:

$$8\pi G_N \rho = \frac{F'}{r'^2 r^2}. \quad (1.63)$$

Thus, we have obtained the *Tolman solution* for spherically symmetric, inhomogeneous dust:

$$ds^2 = -d\tau^2 + \left(\frac{\partial r}{\partial R}\right)^2 \frac{dR^2}{1 - \varepsilon f^2(R)} + r^2(\tau, R)(d\theta^2 + \sin^2 \theta d\phi^2), \quad (1.64)$$

$$8\pi G_N \rho(\tau, R) = \frac{F'(R)}{r^2 \frac{\partial r}{\partial \rho}}. \quad (1.65)$$

### 1.3.2 Oppenheimer-Snyder model

In this model, we require that the mass density  $\rho$  does not depend on the radial coordinate  $R$  and assume the function  $r(\tau, R)$  is of the form

$$r(\tau, R) = K(\tau) R \quad (1.66)$$

where  $K(\tau)$  is a scaling factor. These conditions give, from Eqs. (1.57) and (1.63),

$$f(R) = R, \quad F(R) = \frac{8\pi G_N}{3} \rho K^3 R^3, \quad \tau_0 = 0 \quad (1.67)$$

and since  $F$  is a function of  $R$  only, we see that  $\rho K^3$  has to be a constant,

$$\rho(\tau) K^3(\tau) \equiv \tilde{M}. \quad (1.68)$$

With these, the interior solution becomes

$$ds^2 = -d\tau^2 + K^2(\tau) \left[ \frac{dR^2}{1 - \varepsilon R^2} + R^2(d\theta^2 + \sin^2 \theta d\phi^2) \right] \quad (1.69)$$

with

$$K(\eta) = \begin{cases} \frac{1}{6}\kappa\tilde{M}(1 - \cos \eta) & \text{for } \varepsilon = +1 \\ \frac{1}{6}\kappa\tilde{M}\left(\frac{\eta^2}{2}\right) & \text{for } \varepsilon = 0 \\ \frac{1}{6}\kappa\tilde{M}(\cosh \eta - 1) & \text{for } \varepsilon = -1 \end{cases} \quad (1.70)$$

and

$$\tau = \begin{cases} -\frac{1}{6}\kappa\tilde{M}(\eta - \sin \eta) & \text{for } \varepsilon = +1 \\ -\frac{1}{6}\kappa\tilde{M}\left(\frac{\eta^3}{6}\right) & \text{for } \varepsilon = 0 \\ -\frac{1}{6}\kappa\tilde{M}(\sinh \eta - \eta) & \text{for } \varepsilon = -1 \end{cases} \quad (1.71)$$

The metric, Eq.(1.71), suggests that the interior of the collapsing star is a constant curvature space whose radius depends on time. For  $\varepsilon = 0, -1$ , the star contracts from its initial size until it collapses to  $r = 0$ . And for  $\varepsilon = 1$ , the star first expands and then collapses.

#### Matching conditions

The exterior solution of the star is given by the Tolman solution for  $\rho = 0$ , and due to Birkhoff's theorem, this must correspond to the Schwarzschild solution.

Since the surface of the star moves on geodesics, Eq.(1.58) must correspond to the radial geodesic equation of the Schwarzschild metric at  $R = R_S$ . This yields

$$F = 2M. \quad (1.72)$$

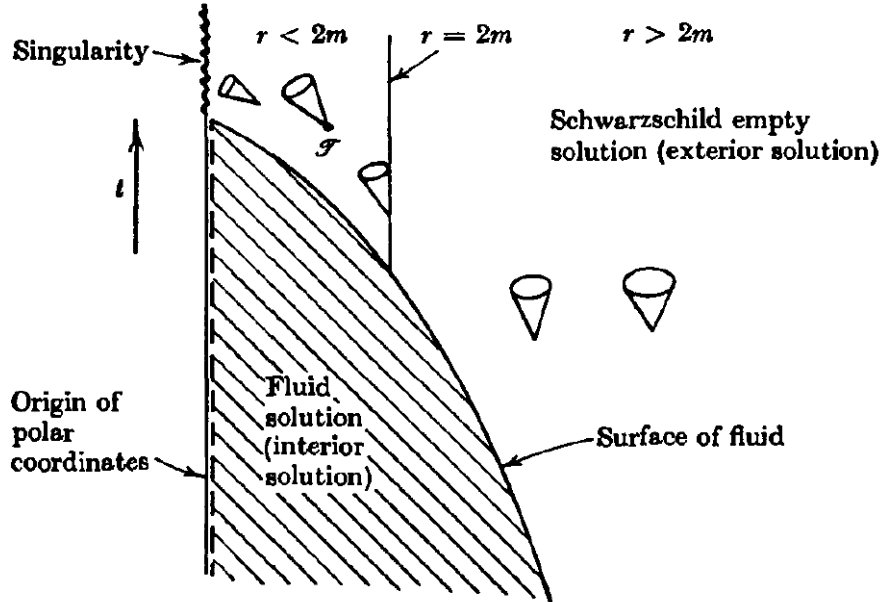


Figure 1.2: Finkelstein diagram of a collapsing spherically symmetric fluid ball. Each point represents a two-sphere. (from[23])

The condition for matching the interior and exterior solutions smoothly is

$$r(\tau, R_S) = K(\tau) R_S. \quad (1.73)$$

This is achieved when

$$\frac{6m}{f^3(R_S)} = \kappa \rho K^3 \quad (1.74)$$

which fixes  $f(R_S) = R_S$ , and we have

$$\kappa \rho K^3 R_S^3 = 6M. \quad (1.75)$$

This condition ensures the continuity of the metric at the surface of the star. It also relates the mass density and radius to the ADM mass of the system.

## 1.4 Black holes

Normally, for a star in static equilibrium, the radius  $r = 2G_N M \equiv R_H$  is far within the interior of the matter. However, a star undergoing a full gravitational collapse will eventually contract past the radius  $R_H$  and approach the  $r = 0$  singularity. Although the  $r = 2G_N M$  singularity of the Schwarzschild metric is merely a coordinate singularity and can be removed by an appropriate coordinate transformation, it is still a crucial aspect of the gravitational collapse and worth a discussion to understand what a collapsing star looks like for an outside observer.

### 1.4.1 Contracting beyond $r = 2G_N M$

By solving the equations for  $\dot{t}$  and  $\dot{r}$ , one obtains (see Appendix B.1)

$$\tau(r) = \frac{2}{3} \frac{1}{\sqrt{2G_N M}} \left( r_0^{3/2} - r^{3/2} \right), \quad (1.76)$$

and

$$\begin{aligned} t(r) = & \frac{2}{3} \frac{1}{\sqrt{2G_N M}} \left( r_0^{3/2} - r^{3/2} + 6Mr_0^{1/2} - 6Mr^{1/2} \right) \\ & + 2G_N M \ln \left[ \frac{\sqrt{r_0} - \sqrt{2G_N M}}{\sqrt{r_0} + \sqrt{2G_N M}} \frac{\sqrt{r} + \sqrt{2G_N M}}{\sqrt{r} - \sqrt{2G_N M}} \right]. \end{aligned} \quad (1.77)$$

Assuming the trajectory starts from  $r_0 \gg 2G_N M$ , behaviour of  $t(r)$  becomes

$$t \simeq \frac{2}{3} \frac{1}{\sqrt{2G_N M}} \left( r_0^{3/2} - r^{3/2} \right) = \tau \quad \text{for } r \gg 2G_N M, \quad (1.78)$$

$$t \simeq -2G_N M \ln(\sqrt{r} - \sqrt{2G_N M}) + \text{const} \quad \text{for } r \simeq 2G_N M. \quad (1.79)$$

Thus, while  $\tau(r)$  is regular,  $t(r)$  diverges as  $r \rightarrow 2G_N M$ . This suggests that, although the particle trajectory crosses  $R_H$  in a *finite amount of proper time*, for an asymptotically inertial observer at  $r \gg R_H$  whose clock measures time  $t$ , it would look like the particle takes an *infinite amount of time*  $t$  to reach  $R_H$ .

To understand this seemingly paradoxical result, we consider a radially infalling probe that emits a signal of frequency  $\omega_s$  at fixed intervals  $\Delta\tau_s$ , and determine the spacetime points of detection of the signals  $(t_n, r_0)$  and their frequencies measured by an asymptotic observer at  $r = r_0$ .

Eq. (B.16) implies that there will be a difference in the observed time interval given by

$$\Delta t_n^{(1)} = \left( 1 - \frac{2G_N M}{r_n} \right)^{-1} \Delta\tau_s. \quad (1.80)$$

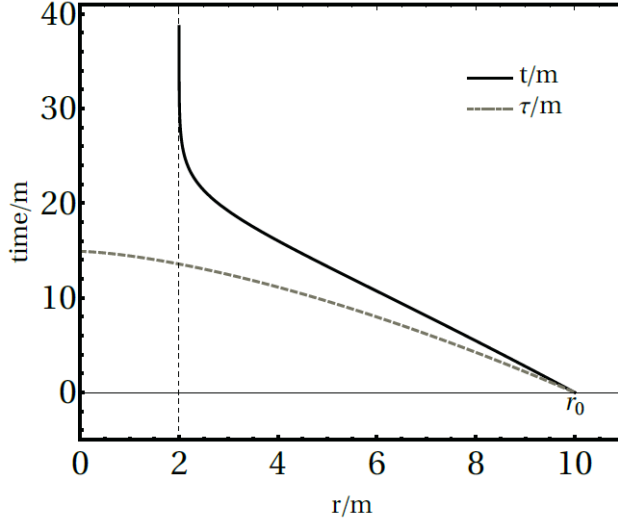


Figure 1.3: Proper time  $\tau$  and coordinate time  $t$ , as functions of  $r$ , for a radially infalling particle in Schwarzschild spacetime (from [24]).

Additionally, the travel time of the signal between two emissions needs to be taken into account, which is, for the asymptotic observer

$$\Delta t_n^{(2)} \equiv t_n - t_{n-1} = \int_{r_n}^{r_0} \frac{dt}{dr} dr - \int_{r_{n-1}}^{r_0} \frac{dt}{dr} dr \simeq \sqrt{\frac{2G_N M}{r_n}} \left(1 - \frac{2G_N M}{r_n}\right)^{-1} \Delta \tau_s \quad (1.81)$$

Adding these up we get a total observed time difference of

$$\Delta t_n = \Delta t_n^{(1)} + \Delta t_n^{(2)} \simeq \left(1 + \sqrt{\frac{2G_N M}{r_n}}\right) \left(1 - \frac{2G_N M}{r_n}\right)^{-1} \Delta \tau_s, \quad (1.82)$$

which means that the time interval between two consecutive signals received by the outside observer will diverge, and the observer will have to wait an asymptotically infinite amount of time between signals as the probe approaches the Schwarzschild radius  $r = 2G_N M$ .

Additionally, looking at the equation for the gravitational redshift with the contribution of the Doppler effect,

$$\omega_n \simeq \omega_s \sqrt{\frac{1 - v_n}{1 + v_n}} \sqrt{1 - \frac{2G_N M}{r_n}}, \quad (1.83)$$

where  $v_n \rightarrow 0$  for  $r_s \rightarrow R_H$ , one can see that the frequency of the signal received by the observer vanishes, i.e.  $\omega_n \rightarrow 0$ .

Thus, we arrive at the conclusion that a spherically symmetric collapsing body will seem to an outside observer as if it is asymptotically slowing down and redshifting and will eventually become so faint that it practically becomes invisible.

## The event horizon

The above results imply that nothing, not even light, can escape the surface  $r = R_H$  once it is crossed. A photon emitted at  $r = R_H$  would spend all of its energy to escape, hence infinitely redshift. For these reasons, the surface of radius  $R_H$  is called the *event horizon*. The physical nature of this surface can be better understood by looking at the properties of constant radius hypersurfaces,  $\mathcal{S}$ , and the behaviour of light cones. For  $r > 2G_NM$ ,  $\mathcal{S}$  is timelike and there exist both ingoing and outgoing light cones. However, for  $r = 2G_NM$ ,  $\mathcal{S}$  is a null hypersurface and the outgoing light cone is stuck at  $r = R_H$ , while for  $r < 2G_NM$ , the light cones are always ingoing. This means that the hypersurfaces with  $r \leq 2G_NM$  can only be crossed in one direction, which is inwards, and supports the identification as an horizon. A region of spacetime surrounded by this event horizon is called a *black hole*.

### 1.4.2 The singularity

As a consequence of what we have discussed so far, it seems that according to general relativity alone, a complete gravitational collapse will inevitably result in a singular final state, where any matter or light ray past the event horizon reaches the point  $r = 0$  in a finite amount of time.

The emergence of such singularities can also be understood by studying the relation between the geodesic congruences and the particular nature of the matter source, as it is described by its energy-momentum tensor. This is what led to the famous singularity theorems of S. W. Hawking and R. Penrose in the 60's and 70's [8, 9] which prove the existence of singularities in general relativity. Before stating the theorem, we first give some necessary definitions.

In general relativity, spacetime is defined as a pair  $(\mathcal{M}, g)$ , i.e. a four-dimensional  $C^\infty$  manifold endowed with a Lorentz metric of signature +2 [23]. The pair  $(\mathcal{M}, g)$  is said to be *geodesically complete* if every geodesic can be extended to arbitrary values of its affine parameter. This is the property that is used in the generally accepted definition of a spacetime singularity. If a spacetime  $(\mathcal{M}, g)$  is timelike or null *geodesically incomplete*, it is said to contain a *singularity*.

Another key point in the proof of the singularity theorems is provided by the so called *Raychaudhuri equation*, which describes the evolution of geodesic congruences. It is given by

$$\frac{d\theta}{d\tau} = -\frac{1}{3}\theta^2 - \sigma_{\mu\nu}\sigma^{\mu\nu} + \omega_{\mu\nu}\omega^{\mu\nu} - R_{\mu\nu}\xi^\mu\xi^\nu \quad (1.84)$$

where  $\theta$  is the *expansion*, the symmetric tensor  $\sigma_{\mu\nu}$  is called the *shear*, the skew-symmetric part  $\omega_{\mu\nu}$  gives the *twist*, and  $\xi^\mu$  is a vector field that is tangent to the congruence of timelike geodesics.

Using the Einstein's equation, the last term in Eq. (1.84) can be written as

$$R_{\mu\nu}\xi^\mu\xi^\nu = 8\pi G_N \left( T_{\mu\nu}\xi^\mu\xi^\nu + \frac{1}{2}T \right). \quad (1.85)$$

where  $T_{\mu\nu}$  is the energy-momentum tensor, and the term  $T_{\mu\nu}\xi^\mu\xi^\nu$  represents the energy density of matter as measured by an observer with four-velocity  $\xi^\mu$ .

There are several conditions in the literature that have been proposed for the energy-momentum tensor of regular matter sources. For any observer with unit timelike four-velocity  $\xi^\mu$ , the conditions in terms of a diagonalisable energy-momentum tensor  $\mathbf{T} = \rho dt \otimes dt + \sum_i p_i dx^i \otimes dx^i$  read

- Weak energy condition:

$$T_{\mu\nu}\xi^\mu\xi^\nu \geq 0 \quad (1.86)$$

This yields  $\rho \geq 0$  and  $\rho + p_i \geq 0$ .

- Strong energy condition:

$$T_{\mu\nu}\xi^\mu\xi^\nu + \frac{1}{2}T \geq 0 \quad (1.87)$$

which gives  $\rho + \sum_i^3 p_i \geq 0$ .

- Dominant energy condition: For all future directed, timelike  $\xi^\mu$ , the vector

$$J^\mu = T^\mu{}_\nu \xi^\nu \quad (1.88)$$

representing a possible flux of energy, should be a future directed timelike or null vector.

Returning to the Raychaudhuri equation, one can see that under the strong energy condition, the right hand side of Eq. (1.84) is always negative. Then, one can write

$$\frac{1}{\theta^2} \left( \frac{d\theta}{d\tau} + \frac{1}{3}\theta^2 \right) \leq 0, \quad (1.89)$$

which, upon integrating, yields

$$\theta^{-1}(\tau) \geq \theta_0^{-1} + \frac{\tau}{3} \quad (1.90)$$

where  $\theta_0$  is the initial value of  $\theta$ . This equation implies that, if the congruence is initially converging, i.e.  $\theta_0 < 0$ , then  $\theta^{-1}(\tau)$  must pass through zero, that is,  $\theta \rightarrow -\infty$ , and the congruence will collapse to a point within a proper time  $\tau \leq 3/|\theta_0|$ .

These results just represent a singularity in the congruence and do not say much about the existence of actual spacetime singularities. In fact, the conclusion is simply that gravity is attractive and will cause particles or light rays to converge to a focusing point, called *caustics*, if they started out moving towards each other.

## Singularity theorems

Before stating the singularity theorems (without proofs), we give one more important definition which is crucial for the understanding of the theorems.

**Definition 1:** A compact, two-dimensional, smooth spacelike submanifold  $\mathcal{T}$ , having the property that the expansion,  $\theta$ , of both ingoing and outgoing sets of future directed null geodesics orthogonal to  $\mathcal{T}$  is everywhere negative, is called a *trapped surface*.

In the extended Schwarzschild solution, all spheres inside the black hole are trapped surfaces. One may think of  $\mathcal{T}$  as being in such a strong gravitational field that even the outgoing light rays are dragged back and are converging. It follows from this fact that trapped surfaces must form in any gravitational collapse whose initial conditions are sufficiently close to the ones for spherical collapse. This has been shown in the following theorem.

**Theorem 1 (Penrose 1965 [8])** *Spacetime  $(\mathcal{M}, g_{\mu\nu})$  cannot be null geodesically complete if it satisfies:*

1.  $R_{\mu\nu}k^\mu k^\nu \geq 0$  for all null vectors  $k^\mu$ ,
2. there is a non-compact Cauchy surface  $\mathcal{S}$  in  $\mathcal{M}$ ,
3. there is a closed trapped surface  $\mathcal{T}$  in  $\mathcal{M}$ .

This theorem tells us that in a gravitational collapse there will occur either a singularity or a Cauchy horizon, and in either case our ability to predict the future breaks down. However, it does not say whether singularities occur in physically realistic solutions. For this, we need the following more general theorem,

**Theorem 2 (Hawking-Penrose 1970 [9])** *Spacetime  $(\mathcal{M}, g_{\mu\nu})$  is not timelike and null geodesically complete if it satisfies the following conditions:*

1.  $R_{\mu\nu}k^\mu k^\nu \geq 0$  for every null and timelike vector  $k^\mu$ ,
2. timelike and null generic conditions are satisfied,
3. there are no closed timelike curves on  $\mathcal{M}$ ,
4. there exists at least one of the following:
  - a compact achronal set without edge,
  - a closed trapped surface,
  - a point  $p$  such that, on every past (or the future) directed null geodesics from  $p$ , the expansion  $\theta$  of the null geodesics emanating from  $p$  becomes negative.

## 1.5 Rotating black holes

The gravitational field of an astronomical body will not be spherically symmetric if the body is rotating. An exact solution of Einstein's equation outside a rotating, axially symmetric, stationary body was found by Roy Kerr in 1963 [25], known as *the Kerr solution*, which we briefly summarise in this section.

### 1.5.1 The Kerr solution

The Kerr solution in Boyer-Lindquist coordinates [26] is given by the metric

$$ds^2 = -dt^2 + \Sigma \left( \frac{dr^2}{\Delta} + d\theta^2 \right) + (r^2 + a^2) \sin^2 \theta d\phi^2 + \frac{2Mr}{\Sigma} (a \sin^2 \theta d\phi - dt)^2, \quad (1.91)$$

where

$$\Delta(r) \equiv r^2 - 2Mr + a^2, \quad (1.92)$$

$$\Sigma(r, \theta) \equiv r^2 + a^2 \cos^2 \theta. \quad (1.93)$$

The parameters  $M$  and  $a \equiv J/M$  represent the ADM mass and angular momentum per unit mass respectively.

Looking at the metric, one can see that the Kerr spacetime is (i) *axisymmetric*, (ii) *stationary*, but (iii) *not static*, i.e. it is not invariant under time reversal. Furthermore, it is also (iv) *asymptotically flat*, and (v) *reduces to Schwarzschild spacetime* in the limit  $a \rightarrow 0$ .

Being stationary and axisymmetric, the Kerr metric admits two Killing vector fields,

$$k^\mu = (1, 0, 0, 0), \quad m^\mu = (0, 0, 0, 1) \quad (1.94)$$

in coordinates  $(t, r, \theta, \phi)$ . Thus, there are two conserved quantities,

$$E \equiv -u^\mu k_\mu, \quad L \equiv u^\mu m_\mu. \quad (1.95)$$

associated to particles in geodesic motion.

### 1.5.2 Horizons

One can also immediately realize that the metric becomes singular at  $\Delta = 0$  and  $\Sigma = 0$ . However, it turns out that the Kretschmann scalar is only singular on  $\Sigma = 0$ , while it is regular on the surfaces where  $\Delta = 0$ . This suggests that these are just coordinate singularities and can be removed by an appropriate coordinate transformation.

To understand where these coordinate singularities occur, we look at the roots of

$$\Delta = r^2 + a^2 - 2G_N Mr = 0. \quad (1.96)$$

- For  $a^2 \leq M^2$ , this equation has two roots

$$r_+ \equiv M + \sqrt{M^2 - a^2}, \quad (1.97)$$

$$r_- \equiv M - \sqrt{M^2 - a^2}, \quad (1.98)$$

so we can write  $\Delta(r) = (r - r_+)(r - r_-)$ . From the norm of the normal vector to the surfaces  $r = r_+$  and  $r = r_-$

$$n^\mu n_\mu = \frac{\Delta}{\Sigma}, \quad (1.99)$$

one can see that these are null hypersurfaces and can be crossed only in one direction, thus identifying as *horizons*, as in the case of a Schwarzschild black hole.

- For  $a^2 > M^2$ , the metric is singular only when  $r = 0$ . Equation (1.96) has no real solution and there is no horizon. In this case, the singularity is said to be “naked”.
- For  $a^2 = M^2$ , the two horizons  $r_+$  and  $r_-$  coincide, and the solution describes an *extremal black hole*.

The two horizons  $r = r_+$  and  $r = r_-$ , which are called the outer horizon and the inner horizon, respectively, divide the spacetime into three regions: (i) For  $r > r_+$ , the constant radius hypersurfaces  $\Sigma$  are timelike and can be crossed both ways. (ii) In the region between the two horizons, i.e.  $r_- < r < r_+$ ,  $\mathcal{S}$  are spacelike and thus a particle crossing the outer horizon can only fall until it reaches the inner horizon. (iii) For  $r < r_-$ , where the  $\Sigma = 0$  singularity is contained,  $\mathcal{S}$  are again timelike and can be crossed in both inwards and outwards.

### 1.5.3 Frame dragging and the ergosphere

One of the peculiar properties of Kerr spacetime is that an observer with zero angular momentum falling towards a Kerr black hole gets dragged along and is forced to co-rotate with the black hole. This can be seen by realizing that the off-diagonal terms in the Kerr metric result in non-zero angular velocity for the observer.

The angular velocity for an observer with four velocity  $u^\mu$  is given by

$$\Omega \equiv \frac{d\phi}{dt} = \frac{u^\phi}{u^t}. \quad (1.100)$$

Since we are considering a zero angular momentum observer, i.e.  $L = u_\phi = 0$ , we can write

$$u_\phi = g_{\phi\phi}u^\phi + g_{t\phi}u^t = 0. \quad (1.101)$$

Using this, and substituting the metric functions, the angular velocity can be written as

$$\Omega = -\frac{g_{t\phi}}{g_{\phi\phi}} = \frac{2Mar}{(r^2 + a^2)^2 - a^2\Delta \sin^2\theta}. \quad (1.102)$$

## The Ergosphere

In Kerr spacetime, the metric function  $g_{tt}$  changes sign at the surfaces

$$r_{S\pm} \equiv M \pm \sqrt{M^2 - a^2 \cos^2 \theta}. \quad (1.103)$$

In Schwarzschild spacetime, these surfaces coincide with the horizon. However, in the Kerr case, the surface  $r_{S+}$  lies outside the outer horizon  $r_+$ . This means that, there is a region outside the horizon, called the *ergoregion*, where the timelike killing vector field  $k^\mu$  becomes spacelike. This forces observers to co-rotate with the black hole and a *static observer cannot exist* even if it has arbitrarily large angular momentum. The surface  $r_{S+}$  is called the *ergosphere*, or sometimes the *stationary limit surface*.

### 1.5.4 The singularity of Kerr spacetime

The curvature singularity of Kerr spacetime occurs on the surface

$$\Sigma = r^2 + a^2 \cos^2 \theta = 0 \quad (1.104)$$

where the Kretschmann scalar diverges. The nature of this singularity is better understood by transforming to *Kerr-Schild coordinates*  $(\bar{t}, x, y, z)$ , where

$$x + iy = (r + ia) \sin \theta \exp \left[ i \int \left( d\phi + \frac{a}{\Delta} dr \right) \right], \quad (1.105)$$

$$z = r \cos \theta, \quad (1.106)$$

$$\bar{t} = -r + \int \left( dt + \frac{(r^2 + a^2)}{\Delta} dr \right). \quad (1.107)$$

With these the metric takes the form

$$\begin{aligned} ds^2 = & -d\bar{t}^2 + dx^2 + dy^2 + dz^2 \\ & + \frac{2mr^3}{r^4 + a^2 z^2} \left( d\bar{t} + \frac{r(xdx + ydy) - a(xdy - ydx)}{r^2 + a^2} + \frac{zdz}{r} \right) \end{aligned} \quad (1.108)$$

where  $r$  is defined implicitly by

$$r^4(x^2 + y^2 + z^2 - a^2)r^2 - a^2 z^2 = 0. \quad (1.109)$$

From Eqs. (1.105, 1.106), one obtains

$$\frac{x^2 + y^2}{r^2 + a^2} + \frac{z^2}{r^2} = 1 \quad (1.110)$$

which shows that surfaces of constant radius  $r$  are confocal ellipsoids for  $r \neq 0$ .

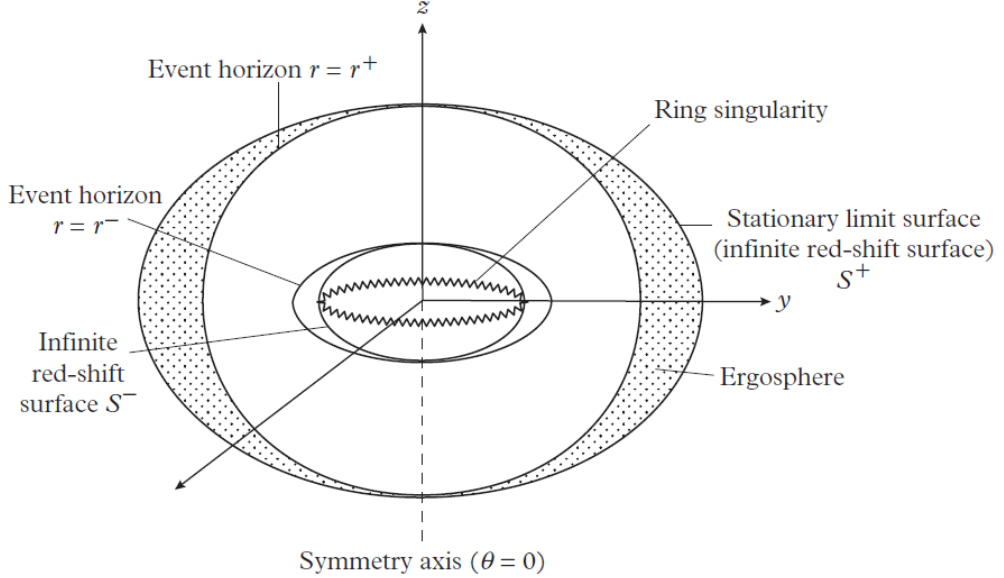


Figure 1.4: Kerr spacetime with  $a^2 < M^2$  (from [27]).

At  $r = 0$  and  $0 < \theta < \pi$ , the ellipsoids degenerate to the disk  $x^2 + y^2 \leq a^2$ . Thus,  $r = 0$  is not a single point but a disk with each value of  $\theta$  corresponding to a circle  $x^2 + y^2 = a^2 \sin^2 \theta$ .

In particular, for  $\theta = \pi/2$ ,  $r = 0$  corresponds to the *ring*

$$x^2 + y^2 = a^2, \quad z = 0, \quad (1.111)$$

which is the boundary of the aforementioned disk. On this ring,  $\Sigma = 0$ , and the Kretschmann scalar actually diverges. Thus, it is a real curvature singularity of the Kerr spacetime, called the *ring singularity*.

# Chapter 2

## Quantum ball of dust

In the literature of regular black holes, one approach of avoiding singularities is to impose regularity conditions inspired by classical physics, e.g. finite effective energy density and scalar invariants [28]. However, these conditions usually fail to remove (or bring back) a seemingly undesirable inner Cauchy horizon. This can be seen in the static spherically symmetric case where  $g_{tt} = -e^\varphi g^{rr}$  with  $\varphi = \varphi(r)$  is a regular function, and

$$g^{rr} = 1 - \frac{2m(r)}{r}. \quad (2.1)$$

For the Schwarzschild vacuum solution, the Misner-Hernandez-Sharp mass function

$$m(r) = 4\pi \int_0^r \rho(x)x^2 dx, \quad (2.2)$$

is equal to the ADM mass  $M$  and is constant. Thus, both  $g_{tt}$  and the Kretschmann scalar diverge for  $r \rightarrow 0$ , suggesting that the tidal forces also diverge towards the centre. If we impose the condition that the proper energy density  $\rho(r)$  to be regular for  $r \rightarrow 0$ , then we get  $m \sim r^3$ . This makes the metric functions and the curvature scalars finite at  $r = 0$ , hence removing the Schwarzschild singularity. However, the relation  $m \sim r^3$  makes  $g_{tt}(0) = e^{\varphi(0)} > 0$ , suggesting that  $g_{tt}$  changes sign twice going inward, which suggests that there must exist a second horizon  $r_-$  inside the outer event horizon  $r_+$ .

In quantum theory, one can impose weaker conditions on the energy density of the source [29]. In particular, we can consider

$$\rho \propto |\Psi|^2, \quad (2.3)$$

where  $\Psi = \Psi(r)$  is the wave function of the fully collapsed matter source. Then, since the wave function must yield finite probability densities, the fundamental requirement becomes that  $\Psi$  needs to be integrable. Thus, we must have

$$m(r) \sim 4\pi \int_0^r |\Psi|^2 x^2 dx < \infty, \quad (2.4)$$

for any  $r < \infty$ . This results in a weaker condition  $\rho \sim r^{-2}$  and  $m \sim r$ , which still ensures that  $m(0) = 0$ . This behaviour of  $m$  both removes the inner Cauchy horizon and replaces the central singularity with an integrable singularity where the curvature scalars and the effective energy-momentum tensor diverge but their volume integrals remain finite [30].

In this chapter, we review a recent approach towards the quantisation procedure of the Oppenheimer-Snyder model of dust collapse, in which the trajectories of the dust particles, which follow the geodesics in the classical theory, are quantised [1, 2]. This approach confirms the expected quantum behaviour for the effective energy density and the mass function in Eq. (2.4). Then the analysis of the inner core of the resulting quantum black hole shows to support the idea that black holes are macroscopic extended objects.

## 2.1 Collapse of a quantum ball of dust

The system we consider is the collapse of a spherically symmetric and isotropic ball of dust, which has a total ADM mass of  $M$  and an areal radius  $R(\tau)$ , where  $\tau$  is the proper time in the comoving frame. During the collapse, the dust particles of proper mass  $\mu$  will fall along the radial geodesics  $r(\tau)$  of the Schwarzschild metric

$$ds^2 = -\left(1 - \frac{2G_N m}{r}\right) dt^2 + \left(1 - \frac{2G_N m}{r}\right)^{-1} dr^2 + r^2 d\Omega^2 \quad (2.5)$$

where  $m(r)$  is the (Misner-Sharp-Hernandez) mass function, which represents the fraction of the total ADM mass inside the radius  $r(\tau)$ , and  $d\Omega^2 = d\theta^2 + \sin^2 \theta d\phi^2$  is the usual line element of a 2-sphere.

The first step is to discretise the ball of dust into  $N$  concentric layers, with inner radius  $r = R_i(\tau)$ , and a spherical core in the centre with mass

$$\mu_0 = \epsilon_0 M, \quad (2.6)$$

where  $\epsilon_i$  is the fraction of the ADM mass in the  $i^{\text{th}}$  layer. Each layer surrounding the core has a thickness  $\Delta R_i = R_{i+1} - R_i$  and carry a mass  $\mu_i = \epsilon_i M$ . Thus, the mass inside a sphere of radius  $r < R_i$  is given by

$$M_i = \sum_{j=0}^{i-1} \mu_j = M \sum_{j=0}^{i-1} \epsilon_j, \quad (2.7)$$

and the total mass is  $M = M_{N+1}$ .

Since each layer of dust will follow the geodesics, the radial geodesic equation

$$\left(\frac{dR_i}{d\tau}\right)^2 - \frac{2G_N M_i}{R_i} = \frac{E_i^2}{\mu} - 1 \quad (2.8)$$

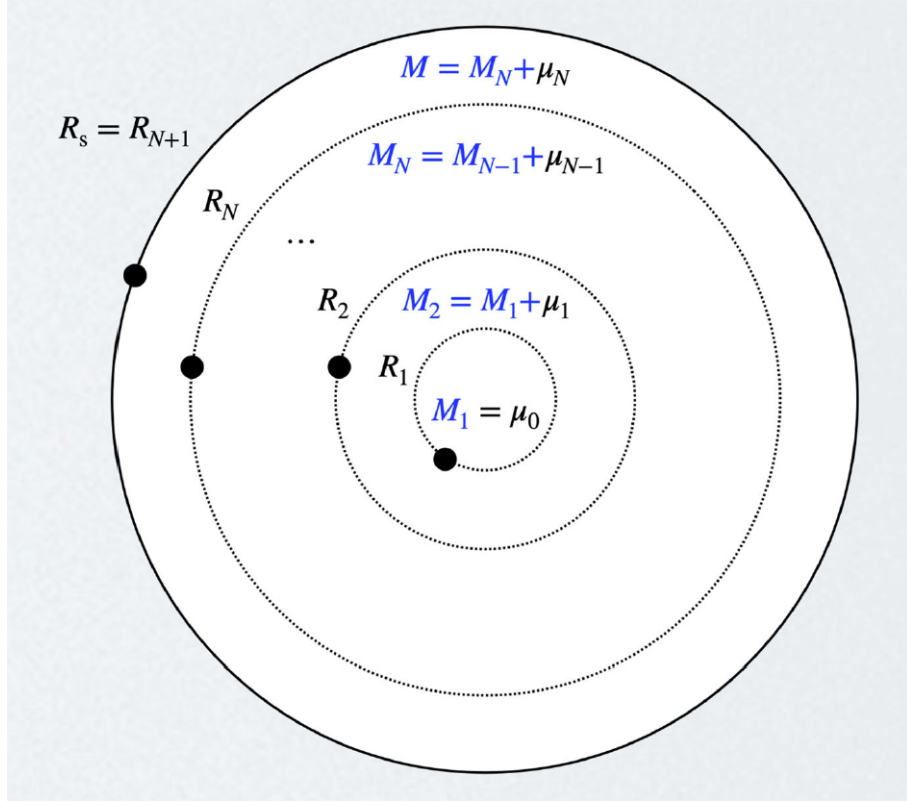


Figure 2.1: The layered structure of the dust ball (from [19])

can be used to study the evolution of the layers, where  $\mu$  is the proper mass of each dust particle, and  $E_i$  is the conserved momentum conjugated to  $t = t_i(\tau)$ . Using the radial momentum<sup>1</sup>  $P_i = \mu \frac{dR_i}{d\tau}$ , conjugated to  $R = R_i(\tau)$ , we can write this equation in the form

$$H_i \equiv \frac{P_i^2}{2\mu} - \frac{G_N \mu M_i}{R_i} = \frac{\mu}{2} \left( \frac{E_i^2}{\mu^2} - 1 \right) \equiv \mathcal{E}_i, \quad (2.9)$$

which is in the same form as the Newtonian equation for energy conservation, and also equivalent to the mass shell condition for the dust layers.

---

<sup>1</sup>The angular momentum conjugated to  $\phi_i = \phi_i(\tau)$  is set to zero since the ball of dust is not spinning.

### 2.1.1 Quantisation

The next step is to employ the canonical quantisation prescription by introducing the momentum operator  $P_i \mapsto \hat{P}_i = -i\hbar\partial_{R_i}$ . With this, and the operator  $\hat{R}_i$ , the canonical commutation relation

$$[\hat{R}_i, \hat{P}_j] = i\hbar\delta_{ij} \quad (2.10)$$

implies that the radius of each layer of the ball satisfies an uncertainty relation<sup>2</sup>

$$\Delta R_i \Delta P_j \gtrsim \hbar = \ell_p m_p \quad (2.11)$$

where  $\Delta O = \langle \hat{O}^2 \rangle - \langle \hat{O} \rangle^2$ . With this prescription, Eq.(2.9) becomes the time-independent Schrödinger equation

$$\hat{H}_i \psi_{n_i} = \left[ -\frac{\hbar^2}{2\mu} \left( \frac{d^2}{dR_i^2} + \frac{2}{R_i} \frac{d}{dR_i} \right) - \frac{G_N \mu M_i}{R_i} \right] \psi_{n_i} = \mathcal{E}_{n_i} \psi_{n_i}. \quad (2.12)$$

which is formally the same as the equation for the s-states of the hydrogen atom. Thus, the Hilbert space of states for the dust particles is spanned by the Hamiltonian eigenfunctions

$$\psi_{n_i}(R_i) = \sqrt{\frac{\mu^6 M_i^3}{\pi \ell_p^3 m_p^9 n_i^5}} \exp\left(-\frac{\mu^2 M_i R_i}{n_i m_p^3 \ell_p}\right) L_{n_i-1}^1\left(\frac{2\mu^2 M_i R_i}{n_i m_p^3 \ell_p}\right), \quad (2.13)$$

where  $L_{n_i-1}^1$  are Laguerre polynomials and  $n_i = 1, 2, \dots$ . The corresponding eigenvalues are

$$\mathcal{E}_{n_i} = -\frac{\mu^3 M_i^2}{2m_p^4 n_i^2}, \quad (2.14)$$

and one can read out a Bohr radius

$$a_i = \frac{\ell_p m_p^2}{\mu M_i}. \quad (2.15)$$

The normalisation of the wave functions (2.13) is defined in the scalar product

$$\langle n_i | n'_i \rangle = 4\pi \int_0^\infty R_i^2 \psi_{n_i}^*(R_i) \psi_{n'_i}(R_i) dR_i = \delta_{n_i n'_i}, \quad (2.16)$$

which makes the Hamiltonian Hermitian when acting on the above spectrum.

The expectation value of the areal radius on these eigenstates is given by

$$\bar{R}_{n_i} \equiv \langle n_i | \hat{R}_i | n_i \rangle = \frac{3m_p^3 \ell_p n_i^2}{2\mu^2 M_i^2}, \quad (2.17)$$

---

<sup>2</sup>The Planck constant  $\hbar$  and the Newton constant  $G_N$  are written in terms of Planck length and mass, i.e.,  $\hbar = \ell_p m_p$  and  $G_N = \ell_p/m_p$ .

with relative uncertainty

$$\frac{\Delta \bar{R}_{n_i}}{\bar{R}_{n_i}} \equiv \frac{\sqrt{\langle n_i | \hat{R}_i^2 | n_i \rangle - \bar{R}_{n_i}^2}}{\bar{R}_{n_i}} = \frac{\sqrt{n_i^2 + 2}}{3n_i}, \quad (2.18)$$

which asymptotes to a minimum of  $1/3$  for  $n_i \rightarrow \infty$ .

### 2.1.2 A lower bound

At first, it seems like the spectrum contains states with infinitesimally small width since  $\bar{R}_1 \sim \ell_p (m_p/M)^3 \ll \ell_p$ , with energy density of the order  $M/\bar{R}_1 \sim (M^{10}/m_p^9)\ell_p^{-3}$ . This state is still indistinguishable from a point-like singularity for any macroscopic black hole and cannot be considered as an alternative to the classical singularity. However, using Eq. (2.5), and assuming that the conserved momentum  $E_i$  remains well defined for all dust particles, i.e.  $E_i^2 \geq 0$ , in the allowed quantum states, we obtain

$$0 \leq \frac{E_i^2}{\mu^2} = 1 + \frac{2\mathcal{E}_i}{\mu} = 1 - \frac{\mu^2 M_i^2}{m_p^4 n_i^2}, \quad (2.19)$$

which gives a lower bound for the single particle principle quantum number

$$n_i \geq \frac{\mu M_i}{m_p^2} \equiv N_i. \quad (2.20)$$

So, the ground state wave function becomes

$$\psi_{N_i}(R_i) = \sqrt{\frac{\mu m_p}{\pi \ell_p^3 M_i^2}} \exp\left(-\frac{\mu R_i}{m_p \ell_p}\right) L_{\frac{\mu M_i}{m_p^2} - 1}^1\left(\frac{2\mu R_i}{m_p \ell_p}\right), \quad (2.21)$$

which is occupied by  $\nu_i$  dust particles in each layer, and from Eq. (2.17) we get

$$\bar{R}_{N_i} = \frac{3}{2} G_N M_i. \quad (2.22)$$

where we require  $M_i$ , and hence  $N_i$  in Eq. (2.16) be such that  $\bar{R}_i \lesssim \bar{R}_{i+1}$ , that is, layer must remain orderly nested.

Using the wave function Eq. (2.21) the effective energy density of each layer can be written as

$$\rho_i = \mu \nu_i |\psi_{N_i}(r)|^2 \simeq \mu \nu_i \left| \psi_{N_i} \left( \frac{3}{2} G_N M_i \right) \right|^2. \quad (2.23)$$

This expression depends on the distribution of  $\nu_i$  particles in each layer, which we do not yet know. In the next section, we see how this is estimated to obtain an expression for the corresponding energy density.

## 2.2 Ground state layers

Since the system consists of dust particles, which by definition only interact gravitationally, the Hilbert space for the entire ball can be assumed to be given by the direct product

$$\mathcal{H} = \bigotimes_{i=1}^N \left( \bigotimes_{k=1}^{\nu_i} \mathcal{H}_i \right) \quad (2.24)$$

of bound eigenstates Eq. (2.13) for  $\nu_i$  particles in each layer. Then, the *global ground state* can be written as the product of single layer ground states

$$|\{\nu_1, N_1\}, \dots, \{\nu_N, N_N\}\rangle = \bigotimes_{i=1}^N |N_i\rangle^{\nu_i}, \quad (2.25)$$

of each layer with  $\nu_i$  particles in their ground state  $|N_i\rangle$ . In order to determine the states  $|N_i\rangle$ , the minimum thickness of the  $i^{th}$  layer of inner radius  $\bar{R}_i$  is assumed to be of the order of  $\overline{\Delta R}_i$  in Eq. (2.18), and the finest possible layering of the dust ball compatible with this quantum description becomes

$$\bar{R}_{i+1} \simeq \bar{R}_i + \overline{\Delta R}_i \gtrsim \frac{4}{3} \bar{R}_i. \quad (2.26)$$

Further assuming  $N_i \gg 1$  for all  $i = 1, \dots, N$ , one finds, using Eq. (2.22),

$$2G_N M_i = \frac{4}{3} \bar{R}_{N_i} \simeq \bar{R}_{N_i} + \overline{\Delta R}_{N_i} \simeq \frac{3}{2} G_N M_{i+1} \quad (2.27)$$

or

$$M_{i+1} \simeq \frac{4}{3} M_i, \quad (2.28)$$

which implies  $\mu_i \simeq M_i/3$ . Then the quantum numbers for the single particle ground states in Eq.(2.25) can be written as

$$N_i \simeq \left( \frac{3}{4} \right)^{N-i+1} \frac{\mu M}{m_p^2}. \quad (2.29)$$

Considering the outermost layer, the quantum number for the particles in the ground state

$$N_S \equiv N_N \simeq \frac{3\mu M}{4m_p^2}, \quad (2.30)$$

can be used to obtain the *global ball radius*:

$$R_S \equiv \bar{R}_{N_S} + \overline{\Delta R}_{N_S} \simeq \frac{3}{2} G_N M. \quad (2.31)$$

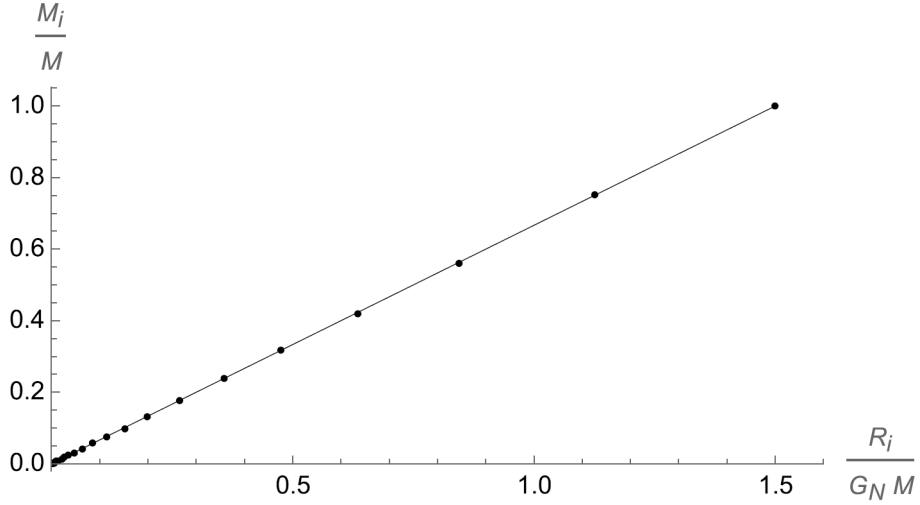


Figure 2.2: Mass function  $M_i$  (dots) for  $N = 100$  layers and its continuous approximation Eq. (2.31) (solid line). The innermost core has radius  $R_1 \simeq 3 \times 10^{-13} R_S$  and mass  $M_1 \simeq 2 \times 10^{-13} M$  (from [2]).

This implies that, since  $R_S < 2G_N M \equiv R_H$ , the ground state of the dust ball can be the core of a black hole. Another important property of this result is that the radius Eq. (2.31) depends only on the mass  $M$ . Therefore, the number of layers  $N$ , in other words, how finely the central region of the ball is described, does not affect the result (2.31). In particular, the innermost core has radius

$$\bar{R}_1 \simeq \left(\frac{3}{4}\right)^N R_S, \quad (2.32)$$

and mass

$$\mu_0 = M_1 \simeq \left(\frac{3}{4}\right)^{N+1} M. \quad (2.33)$$

It is also interesting that, even though the numerical prefactor is not the same as the Bekenstein-Hawking entropy [31], multiplying the integer  $N_S$  by the total number of particles  $M/\mu$ , is qualitatively in agreement with the black hole area quantisation

$$\frac{M}{\mu} N_S \equiv N_G \sim \frac{M^2}{m_p^2} \sim \frac{R_H^2}{\ell_p^2} \quad (2.34)$$

which suggests that the mass and horizon area are quantised, and further supports the results for the dust ball to be described as a single quantum object.

### 2.2.1 Effective energy density and pressures

The crucial result of this work is that it gives a discrete mass function  $M_i$  that grows linearly with the areal radius  $R_i = \bar{R}_{N_i}$  in the collective ground state regardless of the number of layers  $N$  of the ball. Thus, one can introduce a continuous effective energy density

$$\rho \simeq \frac{M}{4\pi R_S r^2} \simeq \frac{m_p}{6\pi \ell_p r^2}, \quad (2.35)$$

such that the mass function

$$m(r) = 4\pi \int_0^r r^2 \rho(r) dr = \frac{2m_p r}{3\ell_p} \quad (2.36)$$

equals the ADM mass  $M$  for  $r = R_S$  (Fig.2.2).

Since the dust particles are in the ground state, they cannot collapse any further and the quantum core is necessarily in equilibrium. Then, corresponding effective pressures can be determined from the Einstein tensor of the isotropic metric

$$\begin{aligned} ds^2 &= -\left(1 - \frac{2G_N M}{r}\right) dt^2 + \left(1 - \frac{2G_N M}{r}\right)^{-1} dr^2 + r^2 d\Omega^2 \\ &\simeq \frac{1}{3} dt^2 - 3 dr^2 + r^2 d\Omega^2, \end{aligned} \quad (2.37)$$

for  $0 \leq r \leq R_S$ , which yields the effective radial pressure

$$p_r \simeq -\frac{m'}{4\pi r^2} \simeq -\rho \quad (2.38)$$

and the tangential pressure (or tension)

$$p \simeq -\frac{m''}{8\pi r} \simeq 0, \quad (2.39)$$

where  $f' \equiv \partial_r f$ . Since the tangential pressure in each layer vanishes, one can deduce that the system is unstable under perturbations of the angular momentum, thus the system can be made to rotate differentially.

From Eq. (2.37) one can see that there is no inner Cauchy horizon inside the ground state core. It should also be noted that the effective metric Eq. (2.37) cannot be used to describe any meaningful motion inside the core, as the matter is in the ground state and cannot evolve further. Therefore, the analysis of geodesics and geometric invariants remains of formal value in the region of the core, where the quantum ground state does not admit a classical approximation. This is reminiscent of bound states of the electrons in the hydrogen atom, which cannot be described in terms of classical trajectories and thus conceptually similar to our case. But even so, the Ricci and Kretschmann scalars

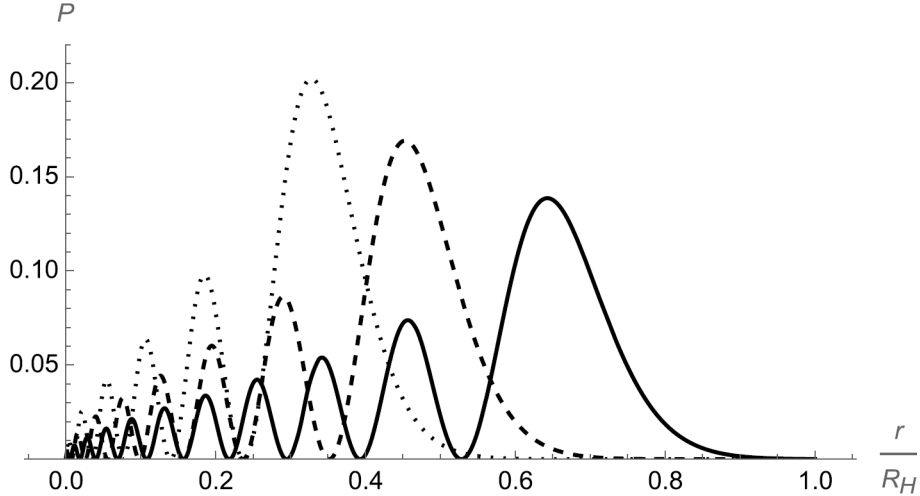


Figure 2.3: Probability density for  $N = 3, \mu = m_p/10, M_3 = 1100\mu$  corresponding to a black hole with  $M \simeq 150m_p$  and  $R_H \simeq 300\ell_p$  (from [2]).

read  $\mathcal{R} \simeq R_{\alpha\beta\gamma\delta}R^{\alpha\beta\gamma\delta} \simeq 64/9r^2$ , whose square roots are integrable, agreeing with the fact that  $\rho \sim |\Psi|^2 \sim r^{-2}$  must be normalisable in quantum theory. Furthermore, the tidal forces remain finite for all  $r$ . Thus,  $r = 0$  can be seen as an integrable singularity since the divergence of geometric invariants does not cause a pathological behaviour of the matter.

As a final note, let us mention a limitation of the assumption of the linear mass function. It can be seen that the outermost layer with thickness  $\overline{\Delta R_N} \simeq R_S/4 \simeq 3G_N M/8$ , contains  $\mu_N/M \simeq 1/4$  of the total mass. So near the surface, a more accurate effective energy density would be of the form  $\rho \simeq \frac{M}{4}|\psi_{N_S}(r)|^2$ . Thus, the mass function is not expected to remain linear near the surface. To see this, we can consider an example with  $N = 3$  layers, plotting the probability densities

$$\mathcal{P}_i = 4\pi r^2 |\psi_{N_i}|^2 = 4\pi \frac{\rho_i(r)}{\mu_i}, \quad (2.40)$$

it turns out that finding a particle of the  $i^{\text{th}}$  layer inside the adjacent layers has a nonzero probability (see Fig. 2.3). This implies that the wave function of the dust particles in a layer overlaps with the ones inside the interior layers. Due to this property, which is neglected in the approximation for the continuous energy density, the actual density is expected to decrease faster from the centre, resulting in different amount of dust in the outermost layer. Thus, requiring a more accurate description of the energy density of the outermost layer, which has just been obtained in [32] recently.

# Chapter 3

## Quantum dust layers of rotating black holes

In this chapter, we first review the analysis done in [3], where the rotational effects have been estimated via perturbation theory. Then, we try to repeat the same analysis considering layers of dust particles in the Kerr geometry.

### 3.1 Rigidly rotating ball with classical angular momentum

In the previous chapter, we dealt with purely radial motion, so we set the conserved angular momenta  $L$  to zero in the geodesic equation. In this section, we look at the effect of rotation on the matter core, which was analysed in [3]. Thus, we include the angular momentum term and compute the perturbative effects for sufficiently slow angular velocity. We consider the outermost ( $N^{\text{th}}$ ) layer as a “one body” with mass  $\mu_N$  and radius  $r = R(\tau)$ , whose evolution is now governed by the geodesic equation

$$\frac{E_\mu^2}{\mu_N^2} - \dot{R}^2 + \frac{2G_N M_N}{R} - \left(1 - \frac{2G_N M_N}{R}\right) \frac{L_\mu^2}{R^2 \mu_N^2} = 1, \quad (3.1)$$

where  $M_N$  is the mass inside the  $N^{\text{th}}$  layer. This can be written in the form, as in Eq. (2.9),

$$\frac{P^2}{2\mu_N} - \frac{G_N \mu_N M_N}{R} + \left(1 - \frac{2G_N M_N}{R}\right) \frac{L_\mu^2}{2\mu_N R^2} = \frac{\mu_N}{2} \left( \frac{E_\mu^2}{\mu_N^2} - 1 \right). \quad (3.2)$$

We consider the case of a rigidly rotating dust ball with angular velocity  $\omega$ . Then, the  $N^{\text{th}}$  layer will have a classical angular momentum

$$L_\mu = \frac{2}{3} \mu_N R^2 \omega \quad (3.3)$$

which we assume to be small enough. Then, we can write the total Hamiltonian as  $H = H_0 + V_L$ , where  $H_0$  is given by Eq. (2.9), and

$$\begin{aligned} V_L &= \left(1 - \frac{2G_N M_N}{R}\right) \frac{L_\mu^2}{2\mu_N R^2} \\ &= \frac{2}{9}\mu_N (R^2 - 2G_N M_N R) \omega^2. \end{aligned} \quad (3.4)$$

Using perturbation theory, one can find the correction to the energy eigenvalues in Eq. (2.14),

$$\Delta\mathcal{E}_{n_i} \equiv \langle n_i | \hat{V}_L | n_i \rangle \simeq \frac{2}{9}\mu_i \bar{R}_{n_i} \left( \frac{10}{9}\bar{R}_{n_i} - 2G_N M_i \right) \omega^2 \quad (3.5)$$

where we assume  $n_i \gg 1$ , and  $\bar{R}_{n_i}$  is given by Eq. (2.17).

For the ground state  $n_i = N_i$ , this becomes

$$\Delta\mathcal{E}_{N_i} \simeq -\frac{1}{9}\mu_i G_N^2 M_i^2 \omega^2 \quad (3.6)$$

Thus, for the  $N^{\text{th}}$  layer, we have

$$\langle N_N | \hat{H} | N_N \rangle = \mathcal{E}_{N_N} + \Delta\mathcal{E}_{N_N} \simeq \mathcal{E}_{N_N} \left( 1 + \frac{2}{9}G_N^2 M_N^2 \omega^2 \right). \quad (3.7)$$

This result is valid only for  $|\Delta\mathcal{E}_{N_N}| \ll |\mathcal{E}_{N_N}|$ , which suggests

$$|\omega| \ll \frac{3}{\sqrt{2}G_N M_N} = \frac{2\sqrt{2}}{G_N M} \equiv \omega_{\max}, \quad (3.8)$$

where we used the fact that the outermost layer encloses a mass  $M_N \simeq 3M/4$ . One can also compute the correction to the ground state quantum number  $N_N$ . To the first order in  $\omega$ , it reads

$$N_N^L \simeq N_N \left( 1 + \frac{1}{9}G_N^2 M_N^2 \omega^2 \right) \simeq N_N \left( 1 + \frac{1}{16}G_N^2 M^2 \omega^2 \right) \quad (3.9)$$

which yields a larger radius

$$\bar{R}_{N_N}^L \simeq \bar{R}_{N_N} \left( 1 + \frac{2}{9}G_N^2 M_N^2 \omega^2 \right) \simeq \bar{R}_{N_N} \left( 1 + \frac{1}{8}G_N^2 M^2 \omega^2 \right). \quad (3.10)$$

This shows that the angular momentum acts as an effective potential barrier and allows for a larger minimum ground state quantum number, thus resulting in a greater radius.

We also note that  $\omega_{\max}$  corresponds to a total angular momentum per unit mass

$$a_{\max} \equiv \frac{L}{M} = \frac{2}{5} \langle N_N | \hat{R}^2 | N_N \rangle \omega_{\max} \quad (3.11)$$

$$\begin{aligned} &\simeq \frac{4}{9} \bar{R}_{N_N}^2 \omega_{\max} \\ &\approx \frac{8}{5} G_N M \end{aligned} \quad (3.12)$$

where we used Eq. (2.18). Then one obtains a maximum value for the ground state quantum number for which the perturbative approach is valid:

$$N_{\max}^L = \frac{3}{2} N = \frac{3\mu_N M_N}{2m_p^2}, \quad (3.13)$$

which corresponds to a maximum radius of

$$\bar{R}_{N_{\max}}^L = 2\bar{R}_{N_N} = 3G_N M_N = \frac{9}{4} G_N M. \quad (3.14)$$

### 3.1.1 Outer geometry

We now look at what the results of the previous section yield when the geometry outside the ball is assumed to be given by the Kerr metric.

Using Eq. (2.18) and Eq. (2.28), one can write the total angular momentum per unit mass of the ball as

$$a = \frac{L}{M} = \frac{2}{5} \langle N | \hat{R}^2 | N \rangle \omega = \frac{9}{16} G_N^2 M^2 \omega \quad (3.15)$$

Then, the outer horizon of the Kerr spacetime (Eq. 1.97) is now located at

$$\begin{aligned} R_+ &= G_N M + \sqrt{G_N^2 M^2 - a^2} \\ &= G_N M \left( 1 + \sqrt{1 - \left( \frac{9}{16} \right)^2 G_N^2 M^2 \omega^2} \right) \\ &\simeq 2G_N M \left( 1 - \frac{1}{12} G_N^2 M^2 \omega^2 \right) \end{aligned} \quad (3.16)$$

while the inner horizon will be at

$$\begin{aligned} R_- &= G_N M - \sqrt{G_N^2 M^2 - a^2} \\ &\simeq G_N M \left[ \frac{(9/16)^2 G_N^4 M^4 \omega^2}{2G_N^2 M^2} \right] \\ &\approx \frac{1}{6} G_N^3 M^3 \omega^2 \ll \bar{R}_{N_i}, \end{aligned} \quad (3.17)$$

from which we can see that the inner horizon is within the dust core, which means that in the perturbative approximation it cannot exist and the geometry will not be the Kerr vacuum.

For the outer horizon  $R_+$ , using Eqns. (3.10) and (3.16), one can find an angular velocity  $\omega_H$ , such that, for

$$\omega > \omega_H \approx \frac{17}{10 G_N M}, \quad (3.18)$$

$R_+$  will also remain inside the core and will not be realised. This suggests that, within the perturbative regime, if the core spins fast enough a black hole will not form at all.

### 3.1.2 Angular momentum quantisation

Considering Eq. (3.9), one should clearly quantise also the angular momentum, since  $N_N$  and  $N_N^L$  should be integers in order to correspond to allowed states in the spectrum (2.17). Thus, we can let  $N_N^L = N_N + n$  where  $n > 0$  is also an integer, and write, using Eq. (3.9)

$$\omega^2 \simeq \omega_N^2 = \frac{16n}{G_N^2 M^2 N_N} \quad (3.19)$$

corresponding to a quantised angular momentum

$$L_n = 12\ell_p m_p \sqrt{N_N n} \quad (3.20)$$

or

$$a_n \equiv \frac{L_n}{M} = 3\ell_p \sqrt{3n}. \quad (3.21)$$

Using these results one can also deduce that the outer horizon area should also be quantised, which looks like

$$\mathcal{A}_+ = 4\pi R_+^2 \simeq \mathcal{A}_H \left( 1 - \frac{8n}{3N_N} \right), \quad (3.22)$$

where  $\mathcal{A}_H$  is the horizon area of a Schwarzschild black hole of mass  $M$ . This makes it clear that larger mass (hence larger  $N_N$ ) corresponds to a larger horizon, however, increasing the angular momentum (i.e. increasing  $n$ ) makes the horizon smaller.

On the other hand, increasing  $N_N$  and  $n$  both makes the core radius larger. So there is a critical angular velocity  $\omega_{nc} \simeq \omega_H$ ,

$$n_c \approx \frac{3N_N}{17} \quad (3.23)$$

above which the core is larger than the horizon and the system is not a black hole.

## 3.2 General relativistic treatment

Now, instead of treating the rotation as a perturbation to the quantum system in the static Schwarzschild geometry, we will examine the same system directly in Kerr spacetime and compare the results.

### 3.2.1 Rotating geodesics

We consider a layer of dust particles falling freely in Kerr spacetime, where the metric in Boyer-Lindquist coordinates is given by

$$ds^2 = -dt^2 + \frac{2G_N m r}{\Sigma} (a \sin^2 \theta d\phi - dt)^2 + \frac{\Sigma}{\Delta} dr^2 + \Sigma d\theta^2 + (r^2 + a^2) \sin^2 \theta d\phi^2 \quad (3.24)$$

where

$$\Sigma = r^2 + a^2 \cos^2 \theta \quad (3.25)$$

and

$$\Delta = r^2 - 2G_N m r + a^2, \quad (3.26)$$

In the above metric, the constant ADM mass  $M$  is replaced by the mass function  $m(r)$  which represents the mass inside the ellipsoids of coordinate radius  $r$ , and  $a = a(r) = J(r)/m(r)$  is the specific angular momentum on the surface of the same ellipsoid.

Dust particles in this metric will follow timelike geodesics  $x^\mu = x^\mu(\tau)$  governed by the Lagrangian

$$2\mathcal{L} = \dot{t}^2 - \frac{2G_N m r}{\Sigma} (a \sin^2 \theta \dot{\phi} - \dot{t})^2 - \Sigma \left( \frac{\dot{r}^2}{\Delta} + \dot{\theta}^2 \right) - (r^2 + a^2) \sin^2 \theta \dot{\phi}^2 = 1 \quad (3.27)$$

Inverting the expressions for the integrals of motion associated to the two killing vector fields of Kerr spacetime

$$E = \left( 1 - \frac{2G_N m r}{\Sigma} \right) \dot{t} + \frac{2G_N m a r}{\Sigma} \sin^2 \theta \dot{\phi}, \quad (3.28)$$

and

$$L = -\frac{2G_N m a r}{\Sigma} \sin^2 \theta \dot{t} + \left( r^2 + a^2 + \frac{2G_N M a^2 r}{\Sigma} \sin^2 \theta \right) \sin^2 \theta \dot{\phi}, \quad (3.29)$$

yields

$$\dot{t} = \frac{1}{\Delta} \left[ \left( r^2 + a^2 + \frac{2G_N m a^2 r}{\Sigma} \sin^2 \theta \right) E - \frac{2G_N m a r}{\Sigma} L \right] \quad (3.30)$$

$$= E + \frac{4G_N m r [(a^2 + r^2) E + a L]}{(r^2 + a^2 - 2G_N m r)[2r^2 + a^2(1 + \cos 2\theta)]}, \quad (3.31)$$

and

$$\dot{\phi} = \frac{1}{\Delta} \left[ \left( 1 - \frac{2G_Nmr}{\Sigma} \right) \frac{L}{\sin^2 \theta} + \frac{2G_Nmar}{\Sigma} E \right] \quad (3.32)$$

$$= \frac{4G_NmarE + 2a^2L}{(r^2 + a^2 - 2G_Nmr)[2r^2 + a^2(1 + \cos 2\theta)]} - \frac{2L}{[2r^2 + a^2(1 + \cos 2\theta)] \sin^2 \theta}. \quad (3.33)$$

In the following, we assume that the dust particles in a layer on the surface of an ellipsoid of radial coordinate  $r = r(\tau)$  co-rotate with the geometry and therefore have  $L = 0$ . Then, from Eq. (3.23) we have

$$\left( r^2 + a^2 + \frac{2G_Nma^2r}{\Sigma} \sin^2 \theta \right) \sin^2 \theta \dot{\phi} = \frac{2G_Nmar}{\Sigma} \sin^2 \theta \dot{t}. \quad (3.34)$$

which gives

$$\dot{t} = E + \frac{2G_Nmr(r^2 + a^2)E}{\Delta\Sigma}, \quad (3.35)$$

and

$$\dot{\phi} = \frac{2G_NmarE}{\Delta\Sigma}. \quad (3.36)$$

With this assumption, the Lagrangian becomes

$$2\mathcal{L}_0 = \left[ E + \frac{2G_Nmr(r^2 + a^2)E}{\Delta\Sigma} \right]^2 - \frac{2G_Nmr(r^2 + a^2)^2E^2}{\Delta^2\Sigma} - \Sigma \left( \frac{\dot{r}^2}{\Delta} + \dot{\theta}^2 \right) + \frac{4G_N^2m^2a^2r^2(r^2 + a^2)E^2 \sin^2 \theta}{\Delta^2\Sigma^2} \quad (3.37)$$

Since the Kerr spacetime is axially symmetric, the trajectories of particles are usually non-planar and the geodesic equations are quite complicated. This makes the system we are considering practically unsolvable. Therefore, we will now consider the cases of radial motion in which the trajectories are planar, that is, along the equatorial plane  $\theta = \pi/2$  and the axis of symmetry  $\theta = 0$ .

### Equatorial motion

For  $\theta = \pi/2$  and  $\dot{\theta} = 0$ , the Lagrangian in Eq. (3.21) reads

$$2\mathcal{L}_0^{\text{eq}} = \frac{1}{r\Delta} \left[ (E^2 - \dot{r}^2)r^3 + a^2(r + 2G_Nm)E^2 \right] = 1, \quad (3.38)$$

which can be written as

$$\frac{1}{2}\dot{r}^2 - \left( \frac{G_Nm}{r} - \frac{a^2}{2r^2} \right) - \left( 1 + \frac{2G_Nm}{r} \right) \frac{a^2E^2}{2r^2} = \frac{1}{2}(E^2 - 1). \quad (3.39)$$

## Axial motion

For  $\theta = \dot{\theta} = 0$ , the Lagrangian becomes

$$2\mathcal{L}_0^{\text{ax}} = \dot{t}^2 \left( 1 - \frac{2G_Nmr}{\Sigma} \right) - \frac{\Sigma}{\Delta} \dot{r}^2 = \frac{\Sigma}{\Delta} (E^2 - \dot{r}^2) = 1 \quad (3.40)$$

where  $\Sigma(r, \theta = 0) = r^2 + a^2$ . Then, we can write

$$\frac{\dot{r}^2}{2} - \frac{G_Nmr}{r^2 + a^2} = \frac{(E^2 - 1)}{2} \quad (3.41)$$

We can also write this as

$$\frac{\dot{r}^2}{2} - \frac{G_Nm}{r} \left( 1 - \frac{a^2}{a^2 + r^2} \right) = \frac{(E^2 - 1)}{2} \quad (3.42)$$

from which we can see that for  $a = 0$ , it describes purely radial motion in Schwarzschild spacetime.

### 3.2.2 Ground state and perturbative spectrum

As in the spherically symmetric case, we discretise the rotating ball into  $N$  comoving, confocal layers by considering an ellipsoidal core of mass  $\mu_0 = \nu_0\mu = \epsilon_0 M$  and coordinate radius  $r = R_1(\tau)$ , which is surrounded by  $N$  layers of inner radius  $r = R_i(\tau)$ , thickness  $\Delta R_i = R_{i+1} - R_i$ , and mass  $\mu_i = \epsilon_i M$ . The gravitational mass inside each ellipsoid  $R_i$  will be denoted by

$$M_i = \sum_{j=0}^{i-1} \mu_j = M \sum_{j=0}^{i-1} \epsilon_j, \quad (3.43)$$

with  $M_1 = \mu_0$  and  $M_{N+1} = M$ . Additionally, we also denote the specific angular momentum at the inner surface of the  $i^{\text{th}}$  layer by  $A_i$ .

Similarly to the spherically symmetric case, we study the evolution of each layer using the fact that dust particles at  $r = R_i(\tau)$  will follow the radial geodesic equation, which can be written as, from Eqs. (3.33, 3.36),

$$H_i \equiv \frac{P_i^2}{2\mu} - \frac{G_N\mu M}{R_i} + W_i = \frac{\mu}{2} \left( \frac{E_i^2}{2} - 1 \right) \quad (3.44)$$

where we let  $P_i = \mu dR_i/d\tau$  be the radial momentum conjugated to  $r = R_i(\tau)$ , and  $E_i$  be the conserved momentum conjugated to  $t = t_i(\tau)$ . We also defined  $W_i$  to be the additional terms in the radial potential, which, for the equatorial motion, reads

$$W_i^{\text{eq}} = \frac{\mu A_i^2}{2R_i^2} \left[ 1 - \left( 1 + \frac{2G_N M_i}{R_i} \right) E_i^2 \right], \quad (3.45)$$

and for axial motion

$$W_i^{\text{ax}} = \frac{\mu G_N M_i A_i^2}{R_i(R_i^2 + A_i^2)}. \quad (3.46)$$

With the canonical quantisation prescription  $P_i \mapsto \hat{P}_i = -i\hbar\partial_{R_i}$ , Eq. (3.38) becomes the time-independent Schrödinger equation

$$\hat{H}_i \psi_{n_i} = \left[ -\frac{\hbar^2}{2\mu} \left( \frac{d^2}{dR_i^2} + \frac{2}{R_i} \frac{d}{dR_i} \right) - \frac{G_N \mu M_i}{R_i} + W_i \right] \psi_{n_i} = \mathcal{E}_{n_i} \psi_{n_i} \quad (3.47)$$

which reduces to the spherically symmetric case for  $W_i \sim a^2 \rightarrow 0$ .

### 3.2.3 Slow-rotation

If we consider  $A_i$  to be small enough, we can use the results of the previous chapter to estimate the corrections to the radial potential. For the equatorial motion, it becomes

$$W_i^{\text{eq}} \simeq \frac{\mu A_i^2}{2\bar{R}_{N_i}^2} \left[ 1 - \left( 1 + \frac{2G_N M_i}{\bar{R}_{N_i}} \right) E_i^2 \right] \simeq \frac{2\mu A_i^2}{9G_N^2 M_i^2} \sim \frac{a^2}{G_N^2 m^2}, \quad (3.48)$$

where we used  $E_i = 0$  for the ground state, and for the axial motion we get

$$W_i^{\text{ax}} \simeq \frac{\mu G_N M_i A_i^2}{\bar{R}_{N_i}(\bar{R}_{N_i}^2 + A_i^2)} \simeq \frac{8\mu A_i^2}{3(9G_N^2 M_i^2 + 4A_i^2)} \sim \frac{a^2}{G_N^2 m^2}. \quad (3.49)$$

If we assume that the geometry is defined by the mass and specific angular momentum of the form  $m \simeq \mu_0 r$  and  $a \simeq \alpha_0 r$ , which is discussed in [29], then these effective potentials are approximately constant. Therefore, they correspond to a correction to the energy eigenvalues of the form

$$\Delta\mathcal{E}_i = -W_i. \quad (3.50)$$

This yields an acceptable estimation only for  $|\Delta\mathcal{E}_i| \ll |\mathcal{E}_i|$ , which amounts to

$$A_N^{\text{eq}} \ll \frac{9}{8} G_N M \quad (3.51)$$

on the equator and

$$A_N^{\text{ax}} \ll 2G_N M \quad (3.52)$$

on the symmetry axis, where we considered the outermost layer. Since  $A_N^{\text{eq}}$  is smaller, we take into consideration only that, and define

$$A_{\max} \equiv \frac{9}{8} G_N M \quad (3.53)$$

With Eq. (3.50), we can find the correction to the ground state quantum number as we did in the previous section. For the equatorial motion we obtain

$$N_{N_i}^{\text{eq}} \simeq N_N \left( 1 + \frac{2A_i^2}{9G_N^2 M_i^2} \right), \quad (3.54)$$

while on the symmetry axis we have

$$N_{N_i}^{\text{ax}} \simeq N_N \left( 1 + \frac{8A_i^2}{3(9G_N^2 M_i^2 + 4A_i^2)} \right). \quad (3.55)$$

Thus, similarly to the previous case, the effective radial potential increases the minimum allowed ground state quantum number, which again, results in a greater radius of the core,

$$\bar{R}_N^{\text{eq}} = \bar{R}_N \left[ 1 + \frac{4A_i^2}{9G_N^2 M_i^2} \right] \quad (3.56)$$

for the equator, and

$$\bar{R}_N^{\text{ax}} = \bar{R}_N \left[ 1 + \frac{16A_i^2}{3(9G_N^2 M_i^2 + 4A_i^2)} \right] \quad (3.57)$$

on the symmetry axis.

## Horizons

The outer horizon will be located at

$$R_+ = 2G_N M \left( 1 - \frac{A_N^2}{4G_N^2 M^2} \right). \quad (3.58)$$

However, we still expect the radius of the core to exceed the outer horizon for some value of  $A_N = A_H$ . We can find the value of  $A_H$  by using Eq. (3.56) and (3.57). For the equatorial motion, we obtain

$$A_H^{\text{eq}} \simeq \sqrt{\frac{63}{73}} G_N M \approx \frac{13}{14} G_N M \quad (3.59)$$

and for the axial motion

$$A_H^{\text{ax}} = \sqrt{\frac{108}{208}} G_N M \approx \frac{3}{4} G_N M. \quad (3.60)$$

On the other hand, the inner horizon  $R_-$  will remain inside the core for all values of  $A_N$  on the equator, within the perturbative approximation of course, because  $\bar{R}_N^{\text{eq}} = R_-$  has no real solution for  $A$ , which also implies that the core radius is larger than  $R_-$  for all values of  $A_N$ . For the axial motion, the inner horizon seems to exceed the core radius at around  $A_N \approx 2G_N M$ , however, this value is beyond the limit  $A_{\text{max}}$ , hence is not a valid result.

### 3.2.4 Quantised specific angular momentum

#### Equatorial motion

As in the case of rigid rotation, we can again deduce from Eqs. (3.54) and (3.55) that the specific angular momentum  $A$  can also be quantised. Then, for the equatorial motion, denoting  $N_N^{\text{eq}} = N_N + n^{\text{eq}}$ , we get

$$\frac{N_N + n^{\text{eq}}}{N_N} - 1 = \frac{n^{\text{eq}}}{N_N} \simeq \left( \frac{2A_i^2}{9G_N^2 M_i^2} \right), \quad (3.61)$$

and find

$$A_n^{\text{eq}} = \frac{3G_N M}{\sqrt{2}} \sqrt{\frac{n^{\text{eq}}}{N_N}}. \quad (3.62)$$

Consequently, the outer horizon radius can be written as

$$R_{n,+}^{\text{eq}} \simeq 2G_N M \left( 1 - \frac{9}{8} \frac{n^{\text{eq}}}{N_N} \right), \quad (3.63)$$

thus, we obtain a quantised horizon area

$$\mathcal{A}_{n,+}^{\text{eq}} \simeq \mathcal{A}_M \left( 1 - \frac{9}{4} \frac{n^{\text{eq}}}{N_N} \right). \quad (3.64)$$

#### Axial motion

Similarly, for the axial motion we obtain

$$\frac{n^{\text{ax}}}{N_N} \simeq \frac{8A_n^2}{3(\frac{81}{16}G_N^2 M^2 + 4A_n^2)}, \quad (3.65)$$

which gives

$$A_n^{\text{ax}} = \frac{9\sqrt{3}}{8\sqrt{2}} G_N M \left( 1 + \frac{3n^{\text{ax}}}{4N_N} \right) \sqrt{\frac{n^{\text{ax}}}{N_N}}. \quad (3.66)$$

This puts the outer horizon radius into the form

$$R_{n,+}^{\text{ax}} = 2G_N M \left[ 1 - \frac{243}{256} \left( 1 + \frac{3n^{\text{ax}}}{4N_N} \right)^2 \frac{n^{\text{ax}}}{N_N} \right], \quad (3.67)$$

which yields the quantised horizon area

$$\mathcal{A}_{n,+}^{\text{ax}} = \mathcal{A}_M \left[ 1 - \frac{243}{128} \left( 1 + \frac{3n^{\text{ax}}}{4N_N} \right)^2 \frac{n^{\text{ax}}}{N_N} \right]. \quad (3.68)$$

Comparing this with Eq. (3.64), we can see that they are approximately equal for  $n^{\text{eq}}, n^{\text{ax}} \gg N_N$ .

# Conclusions

As we have discussed in the first chapter, classical general relativity predicts spacetime singularities through gravitational collapse of sufficiently massive stellar objects. Their existence has been established, at least mathematically, with the famous singularity theorems of Hawking and Penrose. However, it is now also widely accepted that at such scales, general relativity alone cannot describe the full reality, and quantum mechanical effects must be taken into account, even though a complete theory of quantum gravity has not yet been constructed.

There are already several approaches in the literature that attempt to give a quantum mechanical description to the standard collapse models, whose shortcomings have already been discussed in the introduction. Instead, we followed a different procedure which yields promising results towards quantum black holes. We have reviewed the model proposed in [1, 2] in which the collapsed ball of dust was discretised into  $N$  nested layers and their trajectories individually quantised. With this method one finds that there exists ground states for dust particles in each layer, and a collective ground state for the entire core is built self consistently. This then allows one to estimate the expectation value of the global radius of the ball, which turn out to be  $\frac{3}{2}G_NM$  and hence can indeed be the core of a black hole. An interesting point here is that this radius is independent of the number of layers  $N$  of the ball, and only depends on the total mass  $M$ . The crucial result of this model is that the discretised mass function grows linearly with the areal radius in the collective ground state, thus, allowing one to introduce a continuous effective energy density.

Having reviewed the model of quantum dust cores for static, spherically symmetric black holes, we then discussed the effects of rotation on the matter core in the final chapter. First, we considered the case of a rigidly rotating ball with classical angular momentum, as analysed in [3], in which one uses perturbation theory to estimate the corrections to the energy eigenvalues. We saw that, this method yields a larger ground state quantum number and hence corresponds to a larger core radius and a smaller horizon as expected. This also allows one to quantise the angular momentum by introducing an additional quantum number  $n$  and write the corrected ground state quantum number as  $N^L = N + n$ . This further lets us quantise the area of the horizon and see how  $N$  and  $n$  affect it separately. An important result of this analysis was that one can find

a critical angular velocity above which the core becomes larger than the horizon and a black hole does not form at all.

In the final part of the thesis, we have tried to extend this analysis to a fully general relativistic case instead of a classically rotating rigid ball, where we replaced the Schwarzschild geometry with the Kerr metric. However, the geodesic equations of Kerr spacetime are quite complicated, and so a proper analytic solution is practically impossible. Therefore, we instead dealt with a much more simplified case and considered only motion of particles on the equatorial plane and the axis of symmetry. Then, we again took a perturbative approach to estimate the corrected radii and the horizon areas. In the end, we found similar results to the previous case.

In this dissertation, we have only considered a perturbative approach. It seems like the  $1/R^3$  term in the radial potential on the symmetry axis,  $W^{\text{ax}}$ , makes the Schrödinger equation (3.47) unsolvable. However, it might be possible to find an analytic solution for the equatorial motion and see how larger angular momentum affects the quantum core on the equator. Or one can also try to solve Eq. (3.47) numerically and check whether the results are consistent. Furthermore, one would obviously like to develop a more accurate model by considering quantum excitations of standard model fields and their interactions, which could significantly affect the global size of the core and the effective energy density.

# Appendix A

## Curvature quantities

### A.1 Spherically symmetric spacetime

The spherically symmetric spacetime with the general metric

$$ds^2 = -e^{\nu(t,r)}dt^2 + e^{\lambda(t,r)}dr^2 + r^2(d\theta^2 + \sin^2\theta d\phi^2)$$

has the following Christoffel symbols:

$$\begin{aligned} \Gamma_{11}^0 &= \frac{\dot{\lambda}}{2}e^{\lambda-\nu}, & \Gamma_{10}^0 &= \frac{\nu'}{2}, & \Gamma_{00}^0 &= \frac{\dot{\nu}}{2}, \\ \Gamma_{11}^1 &= \frac{\lambda'}{2}, & \Gamma_{10}^1 &= \frac{\dot{\lambda}}{2}, & \Gamma_{22}^1 &= -re^{-\lambda}, \\ \Gamma_{33}^1 &= -r\sin^2\theta e^{-\lambda}, & \Gamma_{00}^1 &= \frac{\nu'}{2}e^{\nu-\lambda}, & \Gamma_{12}^2 &= \frac{1}{r} \\ \Gamma_{33}^2 &= -\sin\theta\cos\theta, & \Gamma_{13}^3 &= \frac{1}{r}, & \Gamma_{23}^3 &= \cot\theta. \end{aligned}$$

with these and the definition of the *Riemann tensor*

$$R^l_{kij} = \Gamma_{kj,i}^l - \Gamma_{ki,j}^l + \Gamma_{mi}^l\Gamma_{kj}^m - \Gamma_{mj}^l\Gamma_{ki}^m, \quad (\text{A.1})$$

the nonzero components of the *Ricci tensor* can be found to be

$$R_{00} = \frac{1}{4}[e^{\nu-\lambda}(2\nu'' + \nu'^2 - \nu'\lambda' + \nu'/r) - (2\ddot{\lambda} + \dot{\lambda}^2 - \dot{\lambda}\dot{\nu})], \quad (\text{A.2})$$

$$R_{11} = \frac{1}{4}[e^{\lambda-\nu}(2\ddot{\lambda} + \dot{\lambda}^2 - \dot{\lambda}\dot{\nu}) - (2\nu'' + \nu'^2 - \nu'\lambda' - \lambda'/r)], \quad (\text{A.3})$$

$$R_{22} = 1 - e^{-\lambda}\left[1 + \frac{r}{2}(\nu' - \lambda')\right], \quad (\text{A.4})$$

$$R_{01} = R_{33}/\sin^2\theta = \frac{\dot{\lambda}}{r}. \quad (\text{A.5})$$

and the *Ricci scalar* is given by

$$\mathcal{R} \equiv R_i^i = -\frac{e^{-\lambda}}{2} \left( 2\nu'' + \nu'^2 - \nu'\lambda' - \frac{4(\nu' - \lambda')}{r} + \frac{4}{r^2} \right) + \frac{2}{r^2} \quad (\text{A.6})$$

### A.1.1 Comoving coordinates

The Christoffel symbols are given by

$$\begin{aligned} \Gamma_{11}^0 &= \frac{\dot{\lambda}}{2} e^\lambda, & \Gamma_{22}^0 &= r\dot{r}, & \Gamma_{33}^0 &= r\dot{r} \sin^2 \theta, \\ \Gamma_{01}^1 &= \frac{\dot{\lambda}}{2}, & \Gamma_{11}^1 &= \frac{\lambda'}{2}, & \Gamma_{22}^1 &= -e^{-\lambda} r' r, \\ \Gamma_{33}^1 &= -e^{-\lambda} r' r \sin^2 \theta, & \Gamma_{02}^2 &= \frac{\dot{r}}{r}, & \Gamma_{12}^2 &= \frac{r'}{r} \\ \Gamma_{33}^2 &= -\sin \theta \cos \theta, & \Gamma_{03}^3 &= \frac{\dot{r}}{r}, & \Gamma_{13}^3 &= \frac{r'}{r}, \\ \Gamma_{23}^3 &= \cot \theta. \end{aligned}$$

which yields the following non-zero Ricci tensor components

$$R_{00} = \frac{\dot{\lambda}^2}{4} + \frac{\ddot{\lambda}}{2} + \frac{2\ddot{r}}{r}, \quad (\text{A.7})$$

$$R_{11} = -\frac{e^\lambda}{4} \left( 2\ddot{\lambda} + \dot{\lambda}^2 + \frac{4\dot{\lambda}\dot{r}}{r} \right) + \frac{(2r'' - r'\lambda')}{r}, \quad (\text{A.8})$$

$$R_{22} = -1 + e^{-\lambda} \left( r''r + r'^2 - \frac{\lambda'r'r}{2} \right) - \ddot{r}r - \dot{r}^2 - \frac{\dot{\lambda}\dot{r}r}{2}, \quad (\text{A.9})$$

$$R_{01} = \frac{2\dot{r}' - \dot{\lambda}r'}{r}. \quad (\text{A.10})$$

Then, the Ricci scalar reads

$$\mathcal{R} = \ddot{\lambda} + \frac{1}{2}\dot{\lambda}^2 + \frac{2\dot{\lambda}\dot{r}}{r} + \frac{4\ddot{r}}{r} + \frac{2}{r^2} (1 + \dot{r}^2 - e^{-\lambda} r'^2) + \frac{2e^{-\lambda}}{r} (\lambda'r' - 2r''). \quad (\text{A.11})$$

# Appendix B

## Geodesics

Geodesic equations can also be derived from the variational principle, which is more convenient for our purposes, by using the fact that they are curves of extremal length. To do this, we vary the action for a massive particle

$$S[x^\mu(\tau)] = m \int_0^\tau \sqrt{-g_{\mu\nu}\dot{x}^\mu\dot{x}^\nu} d\tau' \equiv m \int_0^\tau \sqrt{2T} d\tau', \quad (\text{B.1})$$

and obtain the geodesic equations from the Euler-Lagrange equations. Using the mass shell condition  $g_{\mu\nu}\dot{x}^\mu\dot{x}^\nu = -1$ , the variation of the action reads

$$\delta S = m \delta \int_0^\tau \sqrt{2T} d\tau' = m \int_0^\tau \frac{\delta T}{\sqrt{2T}} d\tau' = m \delta \int_0^\tau T d\tau', \quad (\text{B.2})$$

where  $\tau$  is the proper time of the particle and  $\dot{x}^\mu \equiv \frac{dx}{d\tau}$ . Thus we can define  $T$  to be the Lagrangian  $\mathcal{L}$ , and obtain equations of motion using

$$\frac{d}{d\tau} \left( \frac{\partial \mathcal{L}}{\partial \dot{x}^\mu} \right) = \frac{\partial \mathcal{L}}{\partial x^\mu}, \quad (\text{B.3})$$

which allows us to avoid dealing with the square root.

### B.1 Radial geodesics in Schwarzschild spacetime

The Lagrangian for a massive particle in Schwarzschild geometry is given by

$$\mathcal{L} = \frac{1}{2} \left[ - \left( 1 - \frac{2G_N M}{r} \right) \dot{t}^2 + \left( 1 - \frac{2G_N M}{r} \right)^{-1} \dot{r}^2 + r^2 \dot{\theta}^2 + \sin^2 \theta \dot{\phi}^2 \right] \quad (\text{B.4})$$

Euler-Lagrange equations for the  $\theta$ -component yields

$$\ddot{\theta} = \sin \theta \cos \theta \dot{\phi}^2 - \frac{2}{r} \dot{r} \dot{\theta}. \quad (\text{B.5})$$

Due to the spherical symmetry, we can always choose a certain axis such that the particle trajectory remains on the same plane for any affine parameter. Thus, we pick  $\theta(\tau) = \frac{\pi}{2}$ , which clearly solves the equation of motion.

Since the Schwarzschild metric admits two Killing vector fields, one timelike  $k^\mu = (1, 0, 0, 0)$ , and one spacelike  $m^\mu = (0, 0, 0, 1)$ , one expects two associated conserved quantities, which are given by

$$g_{\mu\nu}k^\mu u^\nu = \left(1 - \frac{2G_N M}{r}\right)\dot{t} = E \quad (\text{B.6})$$

and

$$g_{\mu\nu}m^\mu u^\nu = r^2 \sin^2 \theta \dot{\phi} = L. \quad (\text{B.7})$$

where  $u^\mu \equiv \dot{x}^\mu$  is the four-velocity of the particle, and,  $E$  and  $L$  can be interpreted as energy and angular momentum per unit proper mass respectively. These can be used to obtain equations for  $\dot{t}$  and  $\dot{\phi}$ , which reads ,after choosing  $\theta = \pi/2$  as the orbital plane,

$$\dot{t} = \frac{E}{\left(1 - \frac{2G_N M}{r}\right)}, \quad \text{and} \quad \dot{\phi} = \frac{L}{r^2} \quad (\text{B.8})$$

The radial equation of motion can be obtained more easily by using the mass shell condition

$$2\mathcal{L} = \left(1 - \frac{2G_N M}{r}\right)\dot{t}^2 - \left(1 - \frac{2G_N M}{r}\right)^{-1}\dot{r}^2 - r^2(\dot{\theta}^2 + \sin^2 \theta \dot{\phi}^2) = 1. \quad (\text{B.9})$$

Substituting the expressions for  $\dot{t}$  and  $\dot{\phi}$ , and setting  $\theta = \pi/2$ , this becomes

$$\dot{r}^2 + \left(1 - \frac{2G_N M}{r}\right)\left(1 + \frac{L^2}{r^2}\right) = E^2 \quad (\text{B.10})$$

which yields

$$\dot{r}^2 = E^2 - \left(1 - \frac{2G_N M}{r}\right)\left(1 + \frac{L^2}{r^2}\right), \quad (\text{B.11})$$

which, for purely radial motion, i.e.  $L = 0$ , becomes

$$\dot{r}^2 = \frac{2G_N M}{r} + (E^2 - 1). \quad (\text{B.12})$$

Integrating the expressions for  $\dot{t}$  and  $\dot{r}$ , i.e. Eqs. (B.8) and (B.12), and setting  $E = 1$  one gets

$$\tau(r) = - \int_{r_0}^r dr' \sqrt{\frac{r'}{2G_N M}} = \frac{2}{3} \frac{1}{\sqrt{2G_N M}} \left(r_0^{3/2} - r^{3/2}\right), \quad (\text{B.13})$$

and

$$\begin{aligned}
t(r) &= \int_0^t dt' = - \int_{r_0}^r \frac{dr'}{1 - \frac{2G_N M}{r'}} \sqrt{\frac{r'}{2G_N M}} \\
&= \frac{2}{3} \frac{1}{\sqrt{2G_N M}} \left( r_0^{3/2} - r^{3/2} + 6Mr_0^{1/2} - 6Mr^{1/2} \right) \\
&\quad + 2G_N M \ln \left[ \frac{\sqrt{r_0} - \sqrt{2G_N M}}{\sqrt{r_0} + \sqrt{2G_N M}} \frac{\sqrt{r} + \sqrt{2G_N M}}{\sqrt{r} - \sqrt{2G_N M}} \right]
\end{aligned} \tag{B.14}$$

### Null geodesics

For null geodesics one has

$$\dot{r}^2 + \frac{L^2}{r^2} \left( 1 - \frac{2G_N M}{r} \right) = E^2 \tag{B.15}$$

For radial geodesics, the relevant equations are

$$\frac{dr}{d\tau} = \pm E, \quad \left( 1 - \frac{2G_N M}{r} \right) \frac{dt}{d\tau} = E \tag{B.16}$$

Thus, we have

$$\frac{dr}{dt} = \pm \left( 1 - \frac{2G_N M}{r} \right) \tag{B.17}$$

## B.2 Geodesics of Kerr spacetime

As in the Schwarzschild case, Kerr spacetime admits two Killing vector fields  $k^\mu = (1, 0, 0, 0)$  and  $m^\mu = (0, 0, 0, 1)$ . Using the integrals of motion,

$$E \equiv -u^\mu k_\mu, \quad L \equiv u^\mu m_\mu \quad (\text{B.18})$$

associated to these Killing vector fields, one can obtain equations for  $\dot{t}$  and  $\dot{\phi}$ . In Kerr spacetime  $E$  and  $L$  reads

$$E = \left(1 - \frac{2G_N Mr}{\Sigma}\right)\dot{t} + \frac{2G_N Mar}{\Sigma} \sin^2 \theta \dot{\phi}, \quad (\text{B.19})$$

and

$$L = -\frac{2G_N Mar}{\Sigma} \sin^2 \theta \dot{t} + \left(r^2 + a^2 + \frac{2G_N Ma^2 r}{\Sigma} \sin^2 \theta\right) \sin^2 \theta \dot{\phi}. \quad (\text{B.20})$$

Solving these for  $\dot{t}$  and  $\dot{\phi}$  one obtains

$$\dot{t} = \frac{1}{\Delta} \left[ \left( r^2 + a^2 + \frac{2G_N Ma^2 r}{\Sigma} \sin^2 \theta \right) E - \frac{2G_N Mar}{\Sigma} L \right], \quad (\text{B.21})$$

and

$$\dot{\phi} = \frac{1}{\Delta} \left[ \left( 1 - \frac{2G_N Mr}{\Sigma} \right) \frac{L}{\sin^2 \theta} + \frac{2G_N Mar}{\Sigma} E \right]. \quad (\text{B.22})$$

In the Schwarzschild case, the fourth equation of motion was obtained by using the fact that orbits are planar, and setting  $\theta = \pi/2$ ,  $\dot{\theta} = 0$  along the particle trajectory. Since Kerr spacetime is axisymmetric, orbits in general are not planar, so one cannot pick an arbitrary plane and solve the other three equations. Fortunately, Kerr spacetime admits an additional constant of motion, called the *Carter's constant*, and can be used to solve equations for  $\dot{r}$  and  $\dot{\theta}$ .

The usual approach to find the expressions for  $\dot{r}$  and  $\dot{\theta}$  is to use the *Hamilton-Jacobi method*. Using the Lagrangian of the form  $\mathcal{L} = g_{\mu\nu} \dot{x}^\mu \dot{x}^\nu$  as in (B.3), we define the Hamiltonian of a particle as

$$H(x^\mu, p_\nu) = p_\mu \dot{x}^\mu (p_\nu) - \mathcal{L}(x^\mu, \dot{x}^\mu) = \frac{1}{2} g^{\mu\nu} p_\mu p_\nu \quad (\text{B.23})$$

and look for a function of the coordinates and the parameter  $\lambda$ ,

$$S = S(x^\mu, \lambda) \quad (\text{B.24})$$

which is the solution of the Hamilton-Jacobi equation

$$H \left( x^\mu, \frac{\partial S}{\partial x^\mu} \right) + \frac{\partial S}{\partial \lambda} = 0. \quad (\text{B.25})$$

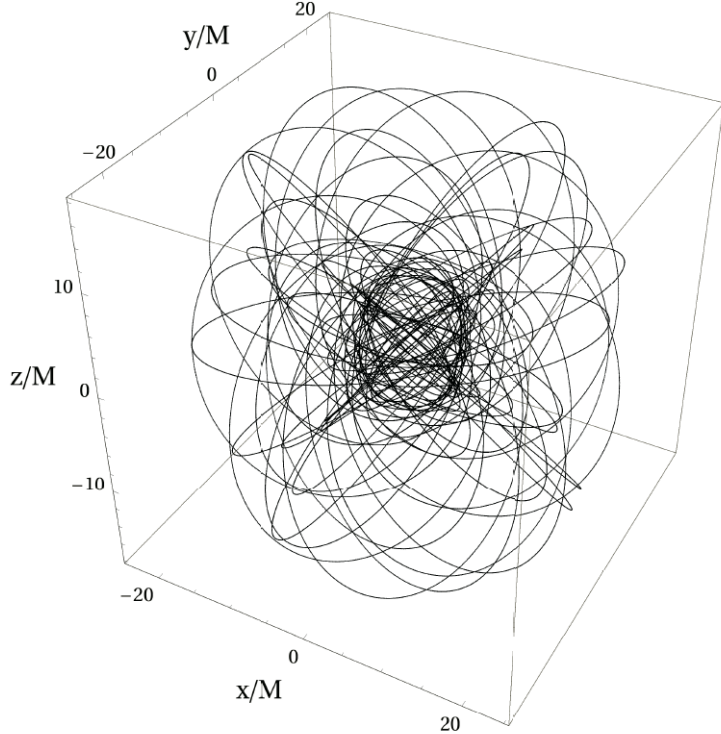


Figure B.1: A trajectory in Kerr spacetime in Cartesian coordinates with  $a = 0.9M$ ,  $E = 0.969$ ,  $L = 2.539$ , and  $C = 6.470$ .

If  $S$  is a complete integral, i.e. it depends on four constants of motion, then

$$\frac{\partial S}{\partial x^\mu} = p_\mu. \quad (\text{B.26})$$

Thus, once the Hamilton-Jacobi equation is solved, the conjugate momenta are found in terms of the four constants and allow one to write the solutions of geodesic equations in closed form.

Using the three constants of motion  $p_t = -E$ ,  $p_\phi = L$  and  $H = \frac{1}{2}g^{\mu\nu}p_\mu p_\nu = -\frac{1}{2}$ , one can write  $S$  as

$$S = -\frac{1}{2}\lambda - Et + L\phi + S^{(r\theta)}(r, \theta) \quad (\text{B.27})$$

where  $S^{(r\theta)}(r, \theta)$  is to be determined.

We look for a separable solution, thus write

$$S = -\frac{1}{2}\lambda - Et + L\phi + S^{(r)}(r) + S^{(\theta)}(\theta). \quad (\text{B.28})$$

Substituting this into Eq. (B.25) one obtains, after some algebra and rearrangements,

$$\begin{aligned} -\Delta \left( \frac{dS^{(r)}}{dr} \right)^2 - r^2 - (L - aE)^2 + \frac{1}{\Delta} [E(r^2 + a^2) - La]^2 \\ = \left( \frac{dS^{(\theta)}}{d\theta} \right)^2 - \cos^2 \theta \left[ (E^2 - 1)a^2 - \frac{L^2}{\sin^2 \theta} \right] \end{aligned} \quad (\text{B.29})$$

The left-hand side of this equation depends only on  $r$ , while the right-hand side depends on  $\theta$ . Thus, we conclude that they must be equal to the same constant,  $\mathcal{C}$ , called the *Carter's constant* [33]. Then, we can define

$$\left( \frac{dS^{(\theta)}}{d\theta} \right)^2 = \cos^2 \theta \left[ (E^2 - 1)a^2 - \frac{L^2}{\sin^2 \theta} \right] + \mathcal{C} \equiv \Theta(\theta), \quad (\text{B.30})$$

$$\left( \frac{dS^{(r)}}{dr} \right)^2 = \frac{1}{\Delta} [-r^2 - (L - aE)^2 - \mathcal{C}] + \frac{1}{\Delta^2} [E(r^2 + a^2) - La]^2 \equiv \frac{R(r)}{\Delta^2}, \quad (\text{B.31})$$

and the solution of the Hamilton-Jacobi equation becomes

$$S = \frac{1}{2}\lambda - Et + L\phi + \int \frac{\sqrt{R}}{\Delta} dr + \int \sqrt{\Theta} d\theta. \quad (\text{B.32})$$

The Carter constant  $\mathcal{C}$  emerges as a separation constant and allows one to solve the geodesic equations of Kerr spacetime completely. It is also important to note that the existence of the Carter constant is not associated to any spacetime isometry, and is a non-trivial property of the Kerr metric.

Given  $S$ , the solution of the Hamilton-Jacobi equations, one can find algebraic expressions for  $\dot{r}$  and  $\dot{\theta}$ . From Eq. (B.26) and the definition of conjugate momentum, one finds

$$\dot{r} = \pm \frac{1}{\Sigma} \sqrt{\Theta}, \quad (\text{B.33})$$

$$\dot{\theta} = \pm \frac{1}{\Sigma} \sqrt{R}. \quad (\text{B.34})$$

Thus, we have obtained four algebraic equations for the components of the four-velocity of the particle in Kerr spacetime.

# Bibliography

- [1] Roberto Casadio. “Quantum dust cores of black holes”. In: *Phys. Lett. B* 843 (2023), p. 138055. DOI: [10.1016/j.physletb.2023.138055](https://doi.org/10.1016/j.physletb.2023.138055). arXiv: [2304.06816 \[gr-qc\]](https://arxiv.org/abs/2304.06816).
- [2] Roberto Casadio. “A quantum bound on the compactness”. In: *Eur. Phys. J. C* 82.1 (2022), p. 10. DOI: [10.1140/epjc/s10052-021-09980-2](https://doi.org/10.1140/epjc/s10052-021-09980-2). arXiv: [2103.14582 \[gr-qc\]](https://arxiv.org/abs/2103.14582).
- [3] Roberto Casadio and Luca Tabaroni. “Slowly rotating quantum dust cores and black holes”. In: *Eur. Phys. J. Plus* 138.1 (2023), p. 104. DOI: [10.1140/epjp/s13360-023-03705-y](https://doi.org/10.1140/epjp/s13360-023-03705-y). arXiv: [2212.05514 \[gr-qc\]](https://arxiv.org/abs/2212.05514).
- [4] J. R. Oppenheimer and H. Snyder. “On Continued gravitational contraction”. In: *Phys. Rev.* 56 (1939), pp. 455–459. DOI: [10.1103/PhysRev.56.455](https://doi.org/10.1103/PhysRev.56.455).
- [5] J. R. Oppenheimer and G. M. Volkoff. “On massive neutron cores”. In: *Phys. Rev.* 55 (1939), pp. 374–381. DOI: [10.1103/PhysRev.55.374](https://doi.org/10.1103/PhysRev.55.374).
- [6] Richard C. Tolman. “Effect of imhomogeneity on cosmological models”. In: *Proc. Nat. Acad. Sci.* 20 (1934), pp. 169–176. DOI: [10.1073/pnas.20.3.169](https://doi.org/10.1073/pnas.20.3.169).
- [7] Richard C. Tolman. “Static solutions of Einstein’s field equations for spheres of fluid”. In: *Phys. Rev.* 55 (1939), pp. 364–373. DOI: [10.1103/PhysRev.55.364](https://doi.org/10.1103/PhysRev.55.364).
- [8] Roger Penrose. “Gravitational collapse and space-time singularities”. In: *Phys. Rev. Lett.* 14 (1965), pp. 57–59. DOI: [10.1103/PhysRevLett.14.57](https://doi.org/10.1103/PhysRevLett.14.57).
- [9] S. W. Hawking and R. Penrose. “The Singularities of gravitational collapse and cosmology”. In: *Proc. Roy. Soc. Lond. A* 314 (1970), pp. 529–548. DOI: [10.1098/rspa.1970.0021](https://doi.org/10.1098/rspa.1970.0021).
- [10] Roberto Casadio. “The scale(s) of quantum gravity and integrable black holes”. In: *Gen. Rel. Grav.* 56.10 (2024), p. 129. DOI: [10.1007/s10714-024-03318-5](https://doi.org/10.1007/s10714-024-03318-5).
- [11] Richard L. Arnowitt, Stanley Deser, and Charles W. Misner. “Dynamical Structure and Definition of Energy in General Relativity”. In: *Phys. Rev.* 116 (1959), pp. 1322–1330. DOI: [10.1103/PhysRev.116.1322](https://doi.org/10.1103/PhysRev.116.1322).

[12] Cenalo Vaz and Louis Witten. “Canonical quantization of spherically symmetric dust collapse”. In: *Gen. Rel. Grav.* 43 (2011), pp. 3429–3449. DOI: [10.1007/s10714-011-1240-4](https://doi.org/10.1007/s10714-011-1240-4). arXiv: [1111.6821 \[gr-qc\]](https://arxiv.org/abs/1111.6821).

[13] Claus Kiefer and Tim Schmitz. “Singularity avoidance for collapsing quantum dust in the Lemaitre-Tolman-Bondi model”. In: *Phys. Rev. D* 99.12 (2019), p. 126010. DOI: [10.1103/PhysRevD.99.126010](https://doi.org/10.1103/PhysRevD.99.126010). arXiv: [1904.13220 \[gr-qc\]](https://arxiv.org/abs/1904.13220).

[14] Włodzimierz Piechocki and Tim Schmitz. “Quantum Oppenheimer-Snyder model”. In: *Phys. Rev. D* 102.4 (2020), p. 046004. DOI: [10.1103/PhysRevD.102.046004](https://doi.org/10.1103/PhysRevD.102.046004). arXiv: [2004.02939 \[gr-qc\]](https://arxiv.org/abs/2004.02939).

[15] Subrahmanyan Chandrasekhar. “The maximum mass of ideal white dwarfs”. In: *Astrophys. J.* 74 (1931), pp. 81–82. DOI: [10.1086/143324](https://doi.org/10.1086/143324).

[16] Jean-Pierre Luminet. “Black holes: A General introduction”. In: *Lect. Notes Phys.* 514 (1998). Ed. by F. W. Hehl, R. J. K. Metzler, and C. Kiefer, pp. 3–34. DOI: [10.1007/978-3-540-49535-2\\_1](https://doi.org/10.1007/978-3-540-49535-2_1). arXiv: [astro-ph/9801252](https://arxiv.org/abs/astro-ph/9801252).

[17] Charles W. Misner and David H. Sharp. “Relativistic equations for adiabatic, spherically symmetric gravitational collapse”. In: *Phys. Rev.* 136 (1964), B571–B576. DOI: [10.1103/PhysRev.136.B571](https://doi.org/10.1103/PhysRev.136.B571).

[18] Walter C. Hernandez and Charles W. Misner. “Observer Time as a Coordinate in Relativistic Spherical Hydrodynamics”. In: *Astrophys. J.* 143 (1966), p. 452. DOI: [10.1086/148525](https://doi.org/10.1086/148525).

[19] Hans A. Buchdahl. “General Relativistic Fluid Spheres”. In: *Phys. Rev.* 116 (1959), p. 1027. DOI: [10.1103/PhysRev.116.1027](https://doi.org/10.1103/PhysRev.116.1027).

[20] Hans Stephani. *Relativity*. Cambridge University Press, 2004.

[21] G. Lemaitre. “The expanding universe”. In: *Annales Soc. Sci. Bruxelles A* 53 (1933), pp. 51–85. DOI: [10.1023/A:1018855621348](https://doi.org/10.1023/A:1018855621348).

[22] H. Bondi. “Spherically symmetrical models in general relativity”. In: *Mon. Not. Roy. Astron. Soc.* 107 (1947), pp. 410–425. DOI: [10.1093/mnras/107.5-6.410](https://doi.org/10.1093/mnras/107.5-6.410).

[23] S.W. Hawking and G.F.R. Ellis. *The Large Scale structure of Space-Time*. Cambridge University Press, 1973.

[24] Valeria Ferrari, Leonardo Gualtieri, and Paolo Pani. *General Relativity and its Applications*. CRC Press, 2020.

[25] Roy P. Kerr. “Gravitational field of a spinning mass as an example of algebraically special metrics”. In: *Phys. Rev. Lett.* 11 (1963), pp. 237–238. DOI: [10.1103/PhysRevLett.11.237](https://doi.org/10.1103/PhysRevLett.11.237).

[26] Robert H. Boyer and Richard W. Lindquist. “Maximal analytic extension of the Kerr metric”. In: *J. Math. Phys.* 8 (1967), p. 265. DOI: [10.1063/1.1705193](https://doi.org/10.1063/1.1705193).

[27] R. d’Inverno. *Introducing Einstein’s relativity*. Oxford University Press, 1992. ISBN: 978-0-19-859686-8.

[28] Raúl Carballo-Rubio et al. “Singularity-free gravitational collapse: From regular black holes to horizonless objects”. In: (Jan. 2023). arXiv: [2302.00028 \[gr-qc\]](https://arxiv.org/abs/2302.00028).

[29] Roberto Casadio, Andrea Giusti, and Jorge Ovalle. “Quantum rotating black holes”. In: *JHEP* 05 (2023), p. 118. DOI: [10.1007/JHEP05\(2023\)118](https://doi.org/10.1007/JHEP05(2023)118). arXiv: [2303.02713 \[gr-qc\]](https://arxiv.org/abs/2303.02713).

[30] Vladimir N. Lukash and Vladimir N. Strokov. “Space-Times with Integrable Singularity”. In: *Int. J. Mod. Phys. A* 28 (2013), p. 1350007. DOI: [10.1142/S0217751X13500073](https://doi.org/10.1142/S0217751X13500073). arXiv: [1301.5544 \[gr-qc\]](https://arxiv.org/abs/1301.5544).

[31] Jacob D. Bekenstein. “Black holes and entropy”. In: *Phys. Rev. D* 7 (1973), pp. 2333–2346. DOI: [10.1103/PhysRevD.7.2333](https://doi.org/10.1103/PhysRevD.7.2333).

[32] L. Gallerani et al. “Mass (re)distribution for quantum dust cores of black holes”. In: *Int. J. Mod. Phys. D* 34.09 (2025), p. 2550035. DOI: [10.1142/S021827182550035X](https://doi.org/10.1142/S021827182550035X). arXiv: [2501.07219 \[gr-qc\]](https://arxiv.org/abs/2501.07219).

[33] B. Carter. “Hamilton-Jacobi and Schrodinger separable solutions of Einstein’s equations”. In: *Commun. Math. Phys.* 10.4 (1968), pp. 280–310. DOI: [10.1007/BF03399503](https://doi.org/10.1007/BF03399503).

[34] Robert M. Wald. *General Relativity*. The University of Chicago Press, 1984.

[35] Steven Weinberg. *Gravitation and Cosmology: Principles and Applications of the General Theory of Relativity*. John Wiley and Sons, 1972.

[36] Subrahmanyan Chandrasekhar. *The mathematical theory of black holes*. Oxford University Press, 1985.

[37] Valeri P. Frolov and Andrei Zelnikov. *Introduction to Black Hole Physics*. Oxford University Press, 2011.

[38] Ya. B. Zel’dovich and I. D. Novikov. *Stars and Relativity*. Dover Publications, 1971.

[39] Richard C. Tolman. *Relativity Thermodynamics and Cosmology*. Dover Publications, 1987.